Review of Data and Formulas for Fusion Cross-sections

Hans–Stephan Bosch

IPP I/252 September 1990

MAX-PLANCK-INSTITUT FÜR PLASMAPHYSIK

8046 GARCHING BEI MÜNCHEN

MAX-PLANCK-INSTITUT FÜR PLASMAPHYSIK

GARCHING BEI MÜNCHEN

Review of Data and Formulas for Fusion Cross-sections

Hans–Stephan Bosch

IPP I/252 September 1990

Die nachstehende Arbeit wurde im Rahmen des Vertrages zwischen dem Max-Planck-Institut für Plasmaphysik und der Europäischen Atomgemeinschaft über die Zusammenarbeit auf dem Gebiete der Plasmaphysik durchgeführt.

REVIEW OF DATA AND FORMULAS FOR FUSION CROSS-SECTIONS

Hans–Stephan Bosch
IPP I/252

Abstract: To interpret fusion rate measurements in present fusion experiments and to predict the fusion performance of future devices it is important to know the fusion cross-sections precisely. Usually, it is not measured data that are used, but analytical parametrizations of the cross-section as a function of the ion energy and of the Maxwellian reactivity as a function of the ion temperature. Since publication of the parametrizations now in use new measurements have been made, and evaluation of the measured data has been improved by applying R-matrix theory.

This report shows that the old parametrizations no longer adequately represent the experimental data and presents new parametrizations for fusion cross-sections and Maxwellian reactivities for the D(d,n)^{3}He-, D(d,p)T-, D(t,n)α-, and D(^{3}He,p)α-reactions.

Contents

1 Introduction

Fusion cross-sections have always been of great interest in plasma physics since they are needed for interpreting fusion rates in plasma diagnostics as well as for predicting fusion rates in reactor design studies. Since about 1945 a lot of measurements have therefore been made on the reactions D(d,n)^{3}He, D(d,p)T, D(t,n)α, and D(^{3}He,p)α, and the experimental data have regularly been reviewed by several authors, resulting in parametrizations or tabulated fit data[JARMIE56A, WANDEL59A, GREENE67A, DUANE72A, STEWART74A] and [PERES79A]. Some of these reviews, however, were restricted to neutron-producing reactions [LISKIEN73A] and [DROSG87A]. Continuous improvement of experimental techniques as well as application of R-matrix theory [HALE79A] resulted in more reliable data and this made discrepancies in the data visible [JARMIE81A, JARMIE86A, BROWN86A]. For most applications, however, analytical approximation formulas are needed to calculate the cross-section as a function of the energy. But the widely used parametrizations[DUANE72A, PERES79A] also involve problems, this being especially true of the most widely used fusion cross-section parametrizations derived by B. H. Duane in 1972 [DUANE72A], which are also listed in the NRL formulary[BOOK87A]. As a consequence, the parametrizations for the Maxwellian reactivity $< \sigma v >$ calculated by M. Hively[HIVELY77A, HIVELY83A] (on the basis of Duane's cross-section formula) and by A. Peres[PERES79A] are not good enough.

New measurements (after 1979) and extensive R-matrix calculations now enable us, however, to derive better parametrizations for fusion cross-sections and Maxwellian reactivities.

A short introduction to the underlying nuclear physics in section 2 is followed, in section 3, by a comparison of the well-known parametrizations with experimental data and R-matrix evaluations. In section 4 a new parametrization for the fusion cross-sections derived from R-matrix evaluations is presented and compared with the old parametrizations, and in section 5 the same is done for the reactivities $< \sigma v >$ in Maxwellian plasmas.

2 Physics background of fusion reactions

2.1 Tunneling through the Coulomb barrier

Two ions approaching each other mainly feel a repulsive force due to Coulomb interaction, unless their separation is smaller than the so-called interaction radius R_i. At shorter distances the attractive nuclear force that binds the two nuclei to a compound nucleus is operational. R_i is of the order of the π-meson Compton wavelength $\hbar/m_\pi c = 1.4 \times 10^{-15}$ m, and it has been found that a good approximation for the interaction radius is $R_i = 1.4\ (A_1^{1/3} + A_2^{1/3}) \times 10^{-15}$ m, where A_1 and A_2 are the atomic weights (in amu) of the interacting particles[CLAYTON68A]. The height of the Coulomb barrier U_b is given in first approximation by the Coulomb potential at R_i, which is

$$U_b = \frac{Z_1 Z_2 e^2}{R_i} = 1.44 \cdot \frac{Z_1 Z_2}{R_i\ [fm]}\ [MeV]. \tag{1}$$

To overcome this barrier directly, the energy available in the center-of-mass system has to be equal to U_b, which is ≈400 keV for the DD-reactions, ≈380 keV for DT and ≈760 keV for D^3He. In fact, the potential has to be modified for contributions of the centrifugal potential as soon as the reacting particles have an angular momentum (i.e. partial waves with $l \geq 1$ are involved). This centrifugal barrier can even be much higher than the Coulomb barrier. With the reduced mass m_r and the angular momentum l the potential $U_l(r)$ is

$$U_l = \frac{l \cdot (l+1)\ \hbar^2}{2 m_r\ r^2} = 20.8 \cdot \frac{l \cdot (l+1)}{r[fm]\ m_r[amu]}\ [MeV]. \tag{2}$$

Fusion reactions, however, already occur for energies much lower than the barrier potential owing to the tunneling of particles through the potential wall. G. Gamov first calculated this effect (for a pure Coulomb potential) for α-decay in 1928 and showed that for energies well below the Coulomb barrier the cross-section is proportional to the tunneling probability :

$$\sigma \sim exp\{-\frac{2\pi Z_1 Z_2 e^2}{\hbar v}\}, \tag{3}$$

with v being the relative velocity of the reacting particles[GAMOV28A]. This can be rearranged to

$$\sigma \sim e^{(-B_G/\sqrt{E})}, \tag{4}$$

where B_G is the Gamov constant

$$B_G = \pi\, \alpha\, Z_1\, Z_2\, \sqrt{2 m_r c^2} \tag{5}$$

with the fine structure constant $\alpha = e^2/\hbar c = 1/137.03604$ and the reduced mass of the particles $m_r c^2$ in keV. Throughout this report E denotes the energy available in the center-of-mass frame. For a particle A with mass m_A hitting the resting particle B the simple relation $E_A = E \cdot (m_A + m_B)/m_B$ holds.

Quantum mechanics shows that the fusion reaction probability is also proportional to a geometrical factor $\pi\lambda^2 \sim 1/E$, where λ is the de Broglie wavelength. The strong energy dependences of this factor and the barrier penetrability motivated the introduction of the astrophysical S-function[BURBIDGE57A, CLAYTON68A] by writing the cross-section as a product of three factors:

$$\sigma = S(E) \cdot \frac{1}{E} \cdot e^{(-B_G/\sqrt{E})}. \tag{6}$$

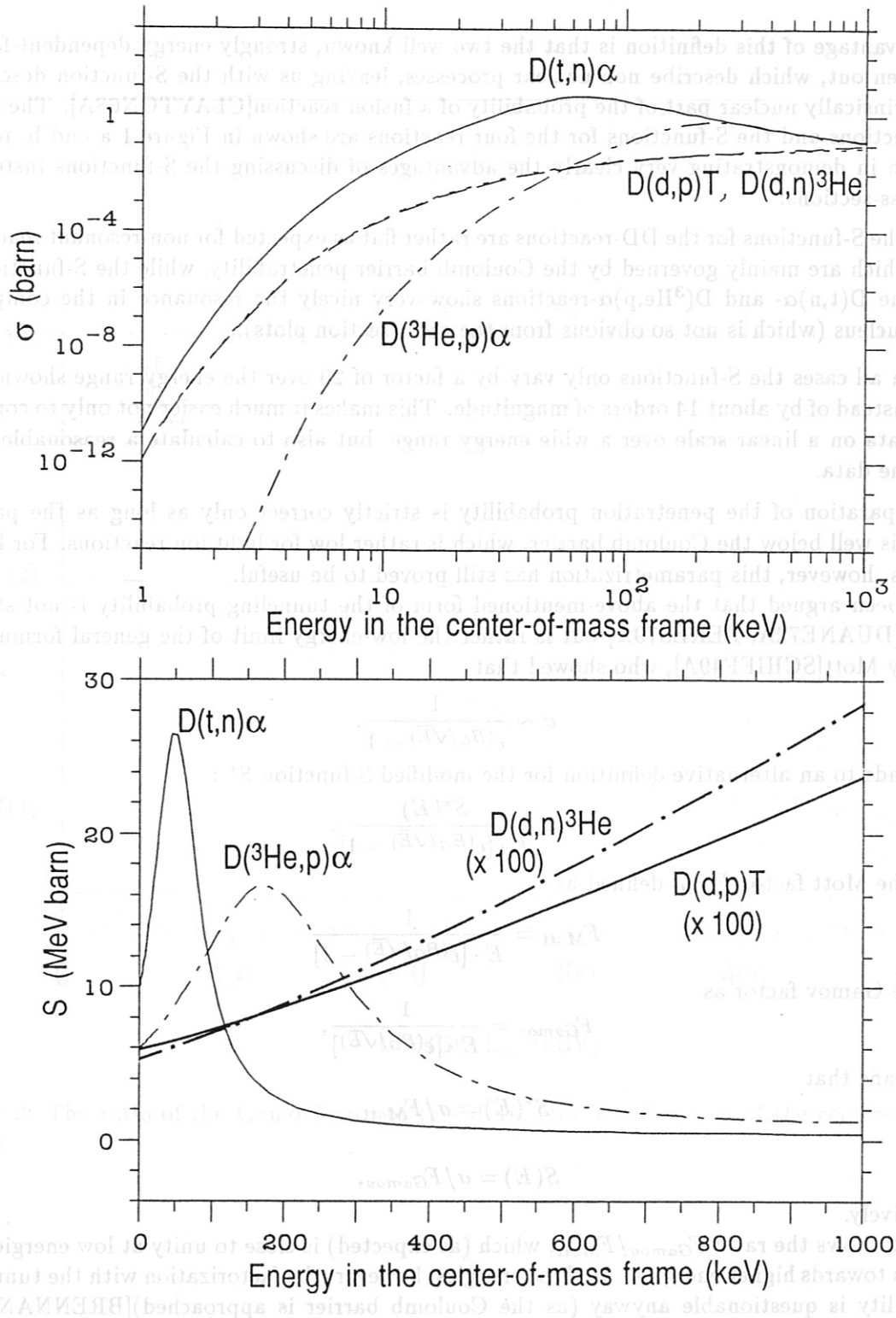

Figure 1: a) Fusion cross-sections for the most important fusion reactions as a function of the center-of-mass energy of the reacting particles. The curves are calculated from Peres's formula. **b)** The S-functions for these reactions as derived from equation 23. For the DD-reactions the data have been multiplied by 100 to improve clarity.

The advantage of this definition is that the two well-known, strongly energy dependent-factors are taken out, which describe non-nuclear processes, leaving us with the S-function describing the intrinsically nuclear part of the probability of a fusion reaction[CLAYTON68A]. The fusion cross-sections and the S-functions for the four reactions are shown in Figure 1 a and b, respectively, n in demonstrating very clearly the advantages of discussing the S-functions instead of the cross-sections:

- The S-functions for the DD-reactions are rather flat as expected for non-resonant reactions, which are mainly governed by the Coulomb barrier penetrability, while the S-functions of the D(t,n)α- and D(^{3}He,p)α-reactions show very nicely the resonance in the compound nucleus (which is not so obvious from the cross-section plots).
- In all cases the S-functions only vary by a factor of 20 over the energy range shown here, instead of by about 14 orders of magnitude. This makes it much easier not only to compare data on a linear scale over a wide energy range, but also to calculate a reasonable fit to the data.

This separation of the penetration probability is strictly correct only as long as the particle energy is well below the Coulomb barrier, which is rather low for light ion reactions. For higher energies, however, this parametrization has still proved to be useful.
It has been argued that the above-mentioned form of the tunneling probability is not strictly correct[DUANE72A, PERES79A] but is rather the low-energy limit of the general formula derived by Mott[SCHIFF49A], who showed that

$$\sigma \sim \frac{1}{e^{(B_G/\sqrt{E})} - 1}. \tag{7}$$

This leads to an alternative definition for the modified S-function S* :

$$\sigma = \frac{S^*(E)}{E \cdot [e^{(B_G/\sqrt{E})} - 1]}. \tag{8}$$

With the Mott factor F_{Mott} defined as

$$F_{Mott} = \frac{1}{E \cdot [e^{(B_G/\sqrt{E})} - 1]} \tag{9}$$

and the Gamov factor as

$$F_{Gamov} = \frac{1}{E \cdot [e^{(B_G/\sqrt{E})}]}, \tag{10}$$

this means that

$$S^*(E) = \sigma / F_{Mott} \tag{11}$$

and

$$S(E) = \sigma / F_{Gamov}, \tag{12}$$

respectively.
Figure 2 shows the ratio F_{Gamov}/F_{Mott}, which (as expected) is close to unity at low energies but changes towards higher energies. At these energies, however, the factorization with the tunneling probability is questionable anyway (as the Coulomb barrier is approached)[BRENNAN58A], but if it is regarded as a mathematical normalization it does not matter which factor is used. Bearing in mind the possibility of integrating the cross-section analytically as is sometimes done in reactivity calculations[BAHCALL66A, MIKKELSEN89A], we use the definition from equation 12 since only this simpler form can be integrated analytically.

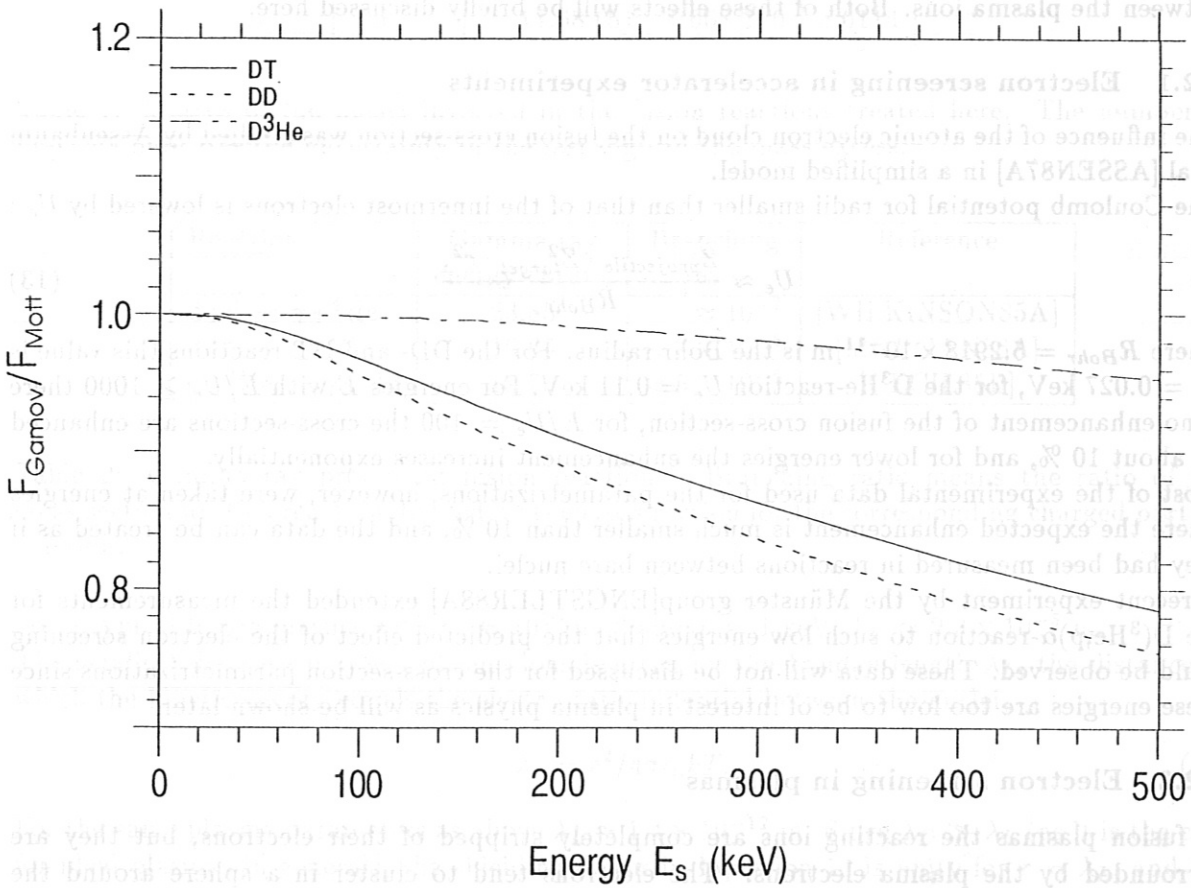

Figure 2: The ratio of the Gamovfactor to the Mottfactor as a function of the center-of-mass energy.

2.2 Screening effect of the electrons

The discussion above was restricted to the ideal case of interaction between bare nuclei. When electrons are involved, however, the Coulomb potential is partially screened, and the effective potential barrier is lower. This was discussed in respect of, for example, the D_2-molecule in the context of "cold fusion"[KOONIN89A].
Electrons are also involved in two cases of interest here, and change the potential: (1) Measurements of fusion cross-sections are done at accelerators where the projectile is an ion but the target is usually atoms or molecules, and (2) the electrons in a plasma influence the potential between the plasma ions. Both of these effects will be briefly discussed here.

2.2.1 Electron screening in accelerator experiments

The influence of the atomic electron cloud on the fusion cross-section was studied by Assenbaum et al.[ASSEN87A] in a simplified model.
The Coulomb potential for radii smaller than that of the innermost electrons is lowered by U_e :

$$U_e \approx \frac{Z_{projectile} \cdot Z_{target}^2 \cdot e^2,}{R_{Bohr}} \tag{13}$$

where $R_{Bohr} = 5.2918 \times 10^{-11}$ m is the Bohr radius. For the DD- and DT-reactions this value is $U_e = 0.027$ keV, for the D^{3}He-reaction $U_e = 0.11$ keV. For energies E with $E/U_e \geq 1000$ there is no enhancement of the fusion cross-section, for $E/U_e = 100$ the cross-sections are enhanced by about 10 %, and for lower energies the enhancement increases exponentially.
Most of the experimental data used for the parametrizations, however, were taken at energies where the expected enhancement is much smaller than 10 %, and the data can be treated as if they had been measured in reactions between bare nuclei.
A recent experiment by the Münster group[ENGSTLER88A] extended the measurements for the D(^{3}He,p)α-reaction to such low energies that the predicted effect of the electron screening could be observed. These data will not be discussed for the cross-section parametrizations since these energies are too low to be of interest in plasma physics as will be shown later.

2.2.2 Electron screening in plasmas

In fusion plasmas the reacting ions are completely stripped of their electrons, but they are surrounded by the plasma electrons. The electrons tend to cluster in a sphere around the nucleus with a radius given by the Debye-length. This in general also leads to screening of the Coulomb potential and enhancement of the fusion rate[SALPETER54A, ICHIMARU82A] and [THIELE86A]. However, this enhancement is only appreciable for very dense plasmas (such as occur in stars), and it does not play a role in fusion plasmas and reactors, as can be shown in a rough estimate:
Owing to the shielding of ions by the surrounding electrons the potential between ions U_p is not a pure Coulomb-potential, but it is attenuated :

$$U_p = -\frac{q}{4\pi\epsilon_0 r} \cdot exp(-r/\lambda_D), \tag{14}$$

where q is the charge, and λ_D is the Debye-length,

$$\lambda_D = \sqrt{\epsilon_0 kT/n_e e^2}. \tag{15}$$

Particle	Mass excess	Mass	
	(MeV)	(keV)	(amu)
n	8.0717 (1)	939 574	1.0087
^{1}H=p	7.2892 (1)	938 280	1.0073
^{2}H=D	13.1363 (2)	1 875 629	2.0136
^{3}H=T	14.9504 (2)	2 808 944	3.0155
^{3}He	14.9317 (2)	2 808 416	3.0149
^{4}He	2.4249 (3)	3 727 411	4.0015
^{5}He	11.39 (5)	4 667 880	5.0111
^{5}Li	11.68 (5)	4 668 170	5.0114

Table 1: Masses of the nuclei involved in the fusion reactions treated here. The number in brackets indicates the uncertainty in the last digit of the mass excess.

Reaction	Gamma ray energy (MeV)	Branching ratio	Reference
d+d $\rightarrow \gamma+^4$He	23.85	$\approx 10^{-7}$	[WILKINSON85A]
d+t $\rightarrow \gamma+^5$He	16.66	$\approx 7 \times 10^{-5}$	[MORGAN86A]
d+^{3}He $\rightarrow \gamma+^5$Li	16.70	$\approx 5 \times 10^{-5}$	[CECIL85B]

Table 2: Gamma ray producing fusion reactions. Branching ratio means the ratio of the cross-section for this reaction divided by the cross-section for the corresponding charged particle reaction.

For a typical fusion plasma with $n_e \approx 10^{20}$ m^{-3} and $T \approx 1$ keV, $\lambda_D \approx 2.3 \times 10^{-5}$ m. The smallest distance between plasma ions is given by the Landau-length λ_L, the distance at which the kinetic energy equals the electrostatic potential between the nuclei,

$$\lambda_L = e^2/4\pi\epsilon_0 kT. \tag{16}$$

For the same plasma parameters as above $\lambda_L \approx 1.4 \times 10^{-12}$ m. Since $\lambda_D \gg \lambda_L$ (as it is the case for ideal plasmas in general), the shielding factor in Equation 14 is unity for $r = \lambda_L$, and the screening of the electrons does not influence the fusion reactions in fusion plasmas. As mentioned before, it is obvious from the Equations 15 and 16, that in stars with non-ideal plasmas, e.g. at low temperatures but very high densities, the situation is completely different.

2.3 The compound nucleus

Once the charged particles have come close enough to feel the attractive nuclear force, a compound nucleus is formed, which has different possibilities to decay, depending on the masses of the reacting particles, compound nucleus and possible reaction products. These nuclear masses can easily be calculated from the tabulated mass excesses[WAPSTRA71A] :

$$m_{nucleus} = A \cdot 1\ amu + mass\ excess - Z \cdot 511\ keV, \tag{17}$$

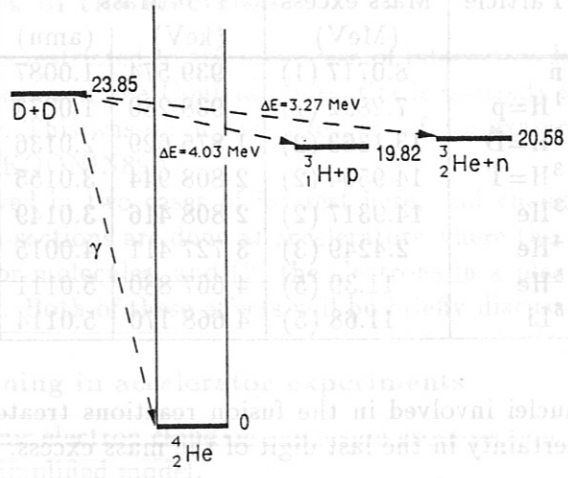

Figure 3: The energy levels of the ^{4}He-system and the other particles involved in the fusion reactions. The corresponding energies are indicated on the energy levels (right). Energies are normalized so that the ground state of ^{4}He is at zero energy. More information on the mass-4 systems can be found in [FIARMAN73A].

where A is the number of nucleons, Z the charge of the nucleus, and 1 amu the atomic mass unit of 931 502 keV. The masses relevant to the reactions considered here are shown in table 1. The energy levels following from them are shown in Figures 3 and 4.

The ^{4}He-nucleus created in the DD-reactions has no excited levels that influence the fusion reaction, although some evidence of such levels has been found (see the review on the physics of the A = 4 system by Fiarman[FIARMAN73A]). The non-resonant reactions are determined only by the Coulomb barrier and the angular momentum barrier penetration. The differential cross-section for these reactions is therefore not isotropic, and the angular distribution strongly depends on the energy available (i.e. the partial waves involved in the reaction). The measurements available on the anisotropy of the differential cross-section have been summarized by Theus et al.[THEUS66A], and more details on the theory of the DD-reactions can be found in[BRENNAN58A, FICK73A].

In the DT-reaction (and the D^{3}He-reaction) a ^{5}He-nucleus (a ^{5}Li-nucleus) is formed. These mass-5 systems are not so well understood, but their properties have been summarized by Ajzenberg-Selove[AJZEN84A]. The two reactions are called mirror reactions, because the number of particles in the compound nucleus is identical, but the ^{5}He-nucleus has 2 protons and 3 neutrons while the ^{5}Li-nucleus has 3 protons and 2 neutrons. These reactions are therefore very similiar, as can be seen in their energy levels. Also both of them have a resonance that is responsible for the rather high cross-sections even at low energies.

The energy level diagrams in Figures 3 and 4 show that other reactions are also possible where the excited compound nucleus emits a γ-quantum. These reactions (which are of great interest in plasma diagnostics[MEDLEY85A, SADLER87A]) are listed in Table 2, but will not be treated further in this report. Details on measurements of the cross-sections (or the branching ratios) can be found in [WILKINSON85A, MORGAN86A, CECIL85C] and in references cited therein.

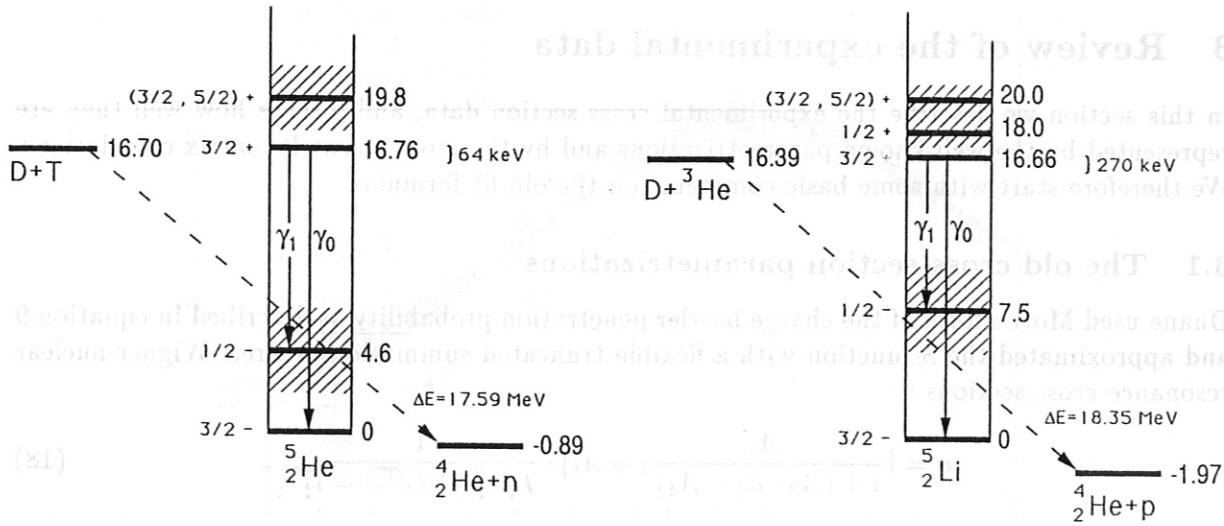

Figure 4: The energy levels of the mass-5 systems,which look very similiar. Both of them have this sharp resonance at 16.76 MeV (^{5}He) and at 16.66 MeV (^{5}Li). The corresponding energies are indicated on the energy levels (right), the total angular momentum and parity J^π on the left side. More information on these systems can be found in [AJZEN84A].

2.4 R-matrix theory

R-matrix theory[LANE58A, STEWART74A, HALE79A, JARMIE84A] provides a mathematical description (and simple parametrization) of nuclear reactions which is independent of the physics model. It is a multi-channel theory that treats different reactions where the total mass and charge of the incident particles are equal (as in T(p,t)P, D(d,n)^{3}He and D(d,p)T) as different "entrance channels". The R-matrix theory describes all the entrance channels and outgoing channels (the different reactions) simultaneously with a single set of parameters.

This, in turn, means that all sorts of experimental data (total fusion cross-sections, differential cross-sections, elastic scattering cross-sections, polarizations etc.) can be used to calculate the R-matrix. Imposing a very large data set strongly improves the reliability of the R-matrix and the cross-sections calculated from these R-matrix parameters.

A simpler explanation is to say that a much larger data set (including data for other reactions) is used to calculate a fit to the cross-section for a specific reaction (in our case the total fusion cross-section).

The calculation of the fusion cross-section from the R-matrix parameters, however, is lengthy and complicated, and it does not seem convenient that everybody should calculate these optimized data again from the original R-matrix. We therefore used cross-sections calculated from the R-matrices by G. M. Hale[HALE79B, HALE86A, HALEPERS] to derive numerical fits to these values, which are presented in section 4.

3 Review of the experimental data

In this section we describe the experimental cross-section data, and discuss how well they are represented by the well-known parametrizations and by the most recent R-matrix calculations. We therefore start with some basic comments on the old fit formulas.

3.1 The old cross-section parametrizations

Duane used Mott's form of the charge barrier penetration probability as described in equation 9 and approximated the S-function with a flexible truncated summation of Breit-Wigner nuclear resonance cross-sections :

$$\sigma = [\frac{A_2}{1+(A_3 \cdot E_l - A_4)^2} + A_5] \cdot \frac{1}{E_l \cdot [e^{(A_1/\sqrt{E_l})} - 1]}. \tag{18}$$

In this formula he uses the laboratory energy E_l of the deuteron. The main problem with his parametrization, however, is that he also considered the constant B_G (see equation 5) as a free parameter (A_1 in his formula) that could be used for the fit. He therefore could not work with the S-values but had to fit the σ-values directly, which vary over many orders of magnitude. This very likely results in a very bad fit at the low energies, where σ is small and the contribution to χ^2 (which is minimized in the fit) is extremely small. It looks as if this problem had not been considered, since the comparison of the experimental data with his parametrization systematically shows a large deviation at the low energies.
A. Peres used the factorization according to equation 8 to derive $S^\star$-values from the experimental data. He then fitted these values with a polynomial in a Padé expansion :

$$S^\star = \frac{A1 + E \cdot (A2 + E \cdot (A3 + E \cdot (A4 + E \cdot A5)))}{1 + E \cdot (B1 + E \cdot (B2 + E \cdot (B3 + E \cdot B4)))}. \tag{19}$$

Here again E is the energy available in the center-of-mass frame. This parametrization shows no systematic deviations from the data but has proved to be a very flexible fit formula. G. Sadler[SADLER87B] therefore used the same procedure as Peres for a fit to the new DT-measurements from Los Alamos[JARMIE84A].

3.2 Data for the D(T,n)α-reaction

The experimental data on this reaction are shown in Figures 5, 6, 7 and 8. Most of these data were taken for energies (in the center-of-mass frame) below 500 kev, with special emphasis on the resonance at $E = 64$ keV (or $E_d = 107$ keV). For the S-function, however, the maximum occurs at $E \sim 48$ keV, as can be seen in these plots.
Duane used for his fit[DUANE72A] the data published by Brolley[BROLLEY51A], Argo[ARGO52A], Conner[CONNER52A], Stratton[STRATTON52A], Arnold[ARNOLD54A], and Hemmendinger[HEMMEN55A], Bame[BAME57A]. Stratton, however, published differential cross-sections only, and we did not calculate the total cross-sections from them. These data have therefore been omitted in this report. A. Peres[PERES79A] used all the data published by Argo, Arnold, Bame, Jarvis[JARVIS53A], and Smith[SMITH72A], and Conner's data for $E \leq 450$ keV only. Smith gave only Legendre coefficients for a fit to the measured values of $d\sigma/d\Omega$ and his data are not shown in this report.

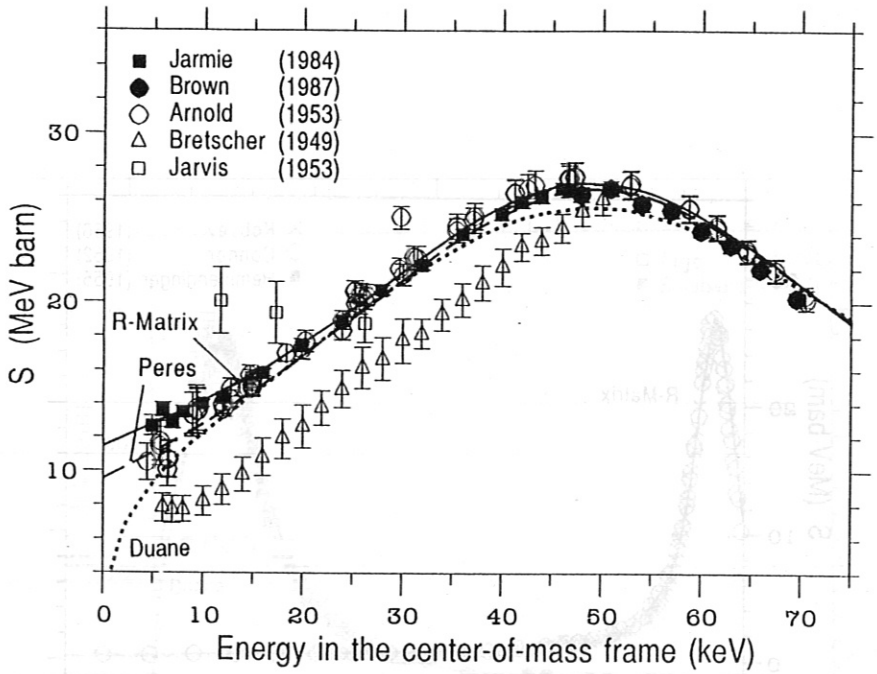

Figure 5: S-values as a function of the energy available in the center-of-mass frame for the DT-reaction. The S-values were derived from the experimental data mentioned in the figure. Bretscher's data are much too low and do not show the maximum, while Jarvis's data do not even follow the trend of the data. The new Los Alamos data confirm quite well the measurements of Arnold et al., except at the very low energies, where Arnold's data are too low.

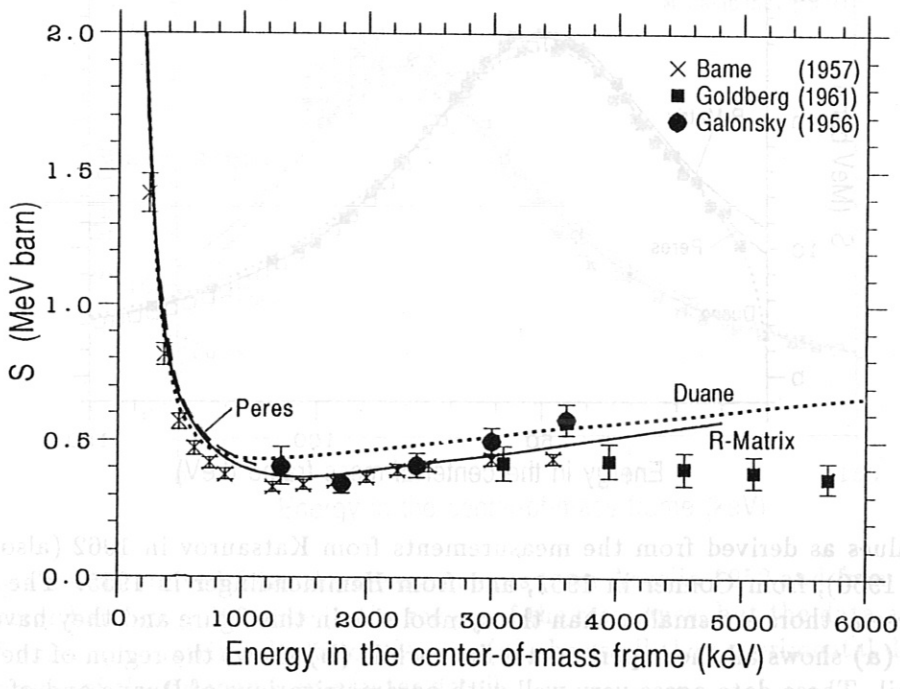

Figure 6: S-values for the DT-reaction in the very high energy region.

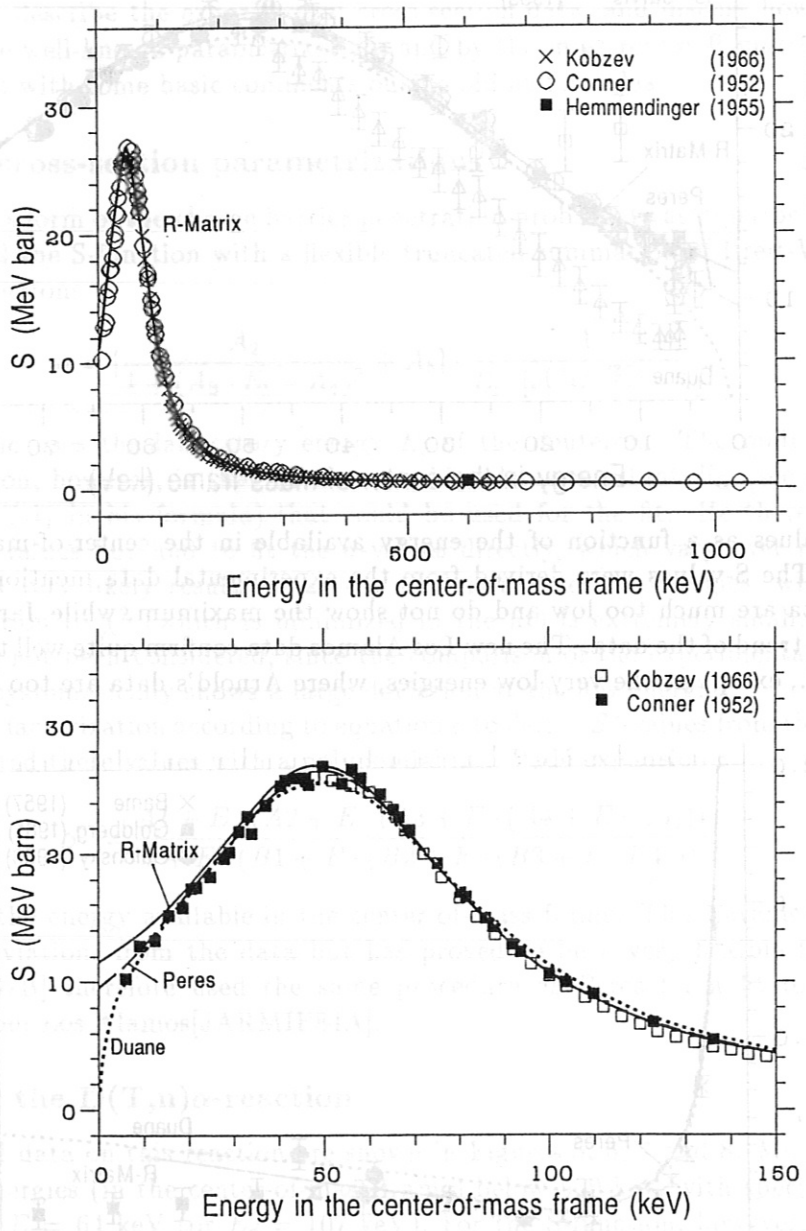

Figure 7: S-values as derived from the measurements from Katsaurov in 1962 (also published by Kobzev in 1966), from Conner in 1952, and from Hemmendinger in 1955. The error bars claimed by these authors are smaller than the symbol size in this figure and they have therefore been omitted. **(a)** shows all the experimental data while **(b)** shows the region of the resonance in greater detail. These data agree very well with parametrizations of Duane and of Peres, and they are a little lower than the R-matrix evaluation.

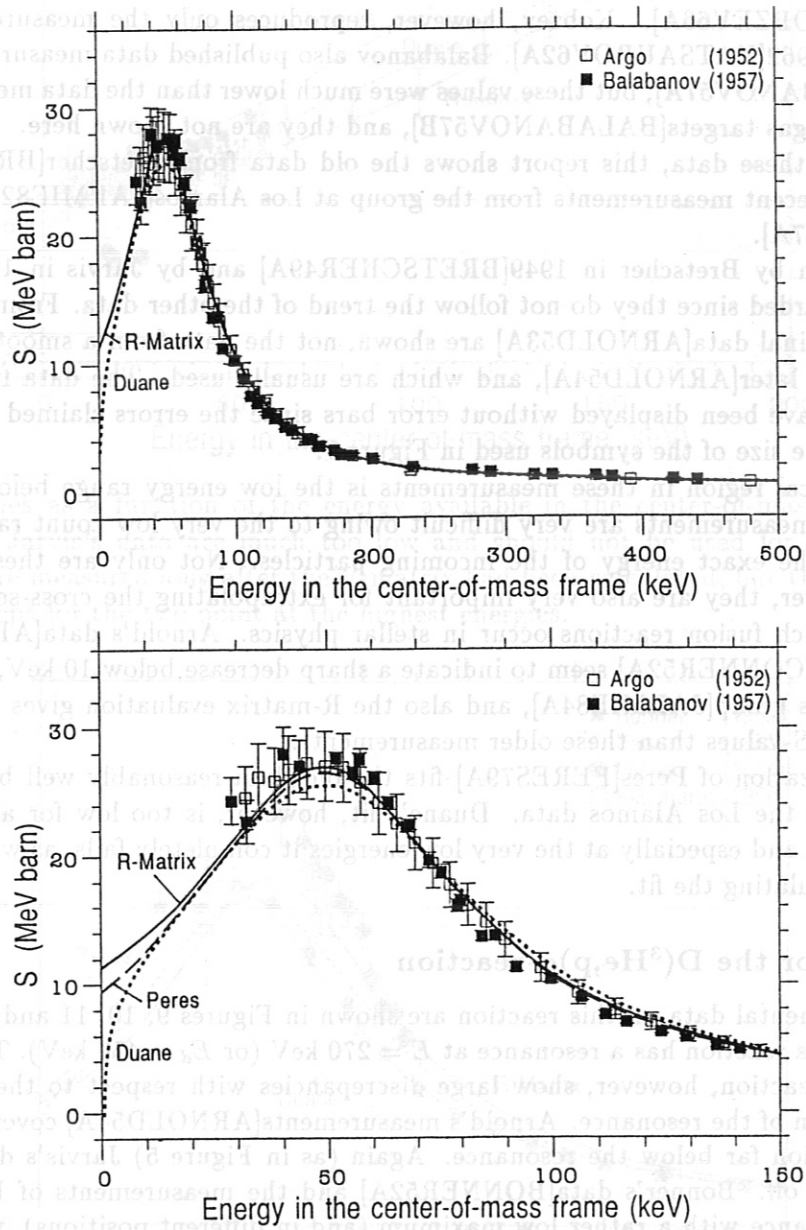

Figure 8: S-values as derived from the measurements from Argo in 1952 and from Balabanov in 1957. The error bars are quite large in the region of the resonance, but the data are even above the values from the R-matrix calculation. Again **(a)** shows all the experimental data while **(b)** shows the region of the resonance in greater detail.

For Liskien's data tables the cross- section data were taken from Argo, Hemmendinger, Bame, Galonsky[GALONSKY56A], Balabanov[BALABANOV57B], and Goldberg[GOLDBERG61A]. Also differential cross-sections in the forward direction $\sigma(0^o)$ were taken from Conner, Arnold, and Kobzev[KOBZEV66A]. Kobzev, however, reproduces only the measurements taken by Katsaurov in 1962[KATSAUROV62A]. Balabanov also published data measured from thick ice targets[BALABANOV57A], but these values were much lower than the data measured from thin solid and from gas targets[BALABANOV57B], and they are not shown here.
In addition to these data, this report shows the old data from Bretscher[BRETSCHER49A], and the most recent measurements from the group at Los Alamos[JARMIE82A, JARMIE84A] and [BROWN87A].
The data taken by Bretscher in 1949[BRETSCHER49A] and by Jarvis in 1953[JARVIS53A] should be discarded since they do not follow the trend of the other data. From Arnold's experiments the original data[ARNOLD53A] are shown, not the data from a smoothed curve which were published later[ARNOLD54A], and which are usually used. The data from Kobzev and from Conner have been displayed without error bars since the errors claimed in the paper are smaller than the size of the symbols used in Figure 7.
The most critical region in these measurements is the low energy range below about 10 keV because these measurements are very difficult owing to the very low count rate and problems in measuring the exact energy of the incoming particles. Not only are these measurements difficult, however, they are also very important for extrapolating the cross-section to the low energies at which fusion reactions occur in stellar physics. Arnold's data[ARNOLD53A] and Conner's data [CONNER52A] seem to indicate a sharp decrease below 10 keV, not observed by the Los Alamos group[JARMIE84A], and also the R-matrix evaluation gives a flat curve with slightly higher S-values than these older measurements.
The parametrization of Peres[PERES79A] fits the old data reasonably well but is a little low compared with the Los Alamos data. Duane's fit, however, is too low for all energies below about 700 keV, and especially at the very low energies it completely fails, as was expected from his way of calculating the fit.

3.3 Data for the D(^{3}He,p)α-reaction

All the experimental data on this reaction are shown in Figures 9, 10, 11 and 12. As was seen in Figure 4, this reaction has a resonance at $E = 270$ keV (or $E_d = 450$ keV). The experimental data for this reaction, however, show large discrepancies with respect to the absolute values and the position of the resonance. Arnold's measurements[ARNOLD54A] covered only the very low energy region far below the resonance. Again (as in Figure 5) Jarvis's data[JARVIS53A] are completely off. Bonner's data[BONNER52A] and the measurements of Kunz[KUNZ55A] showed a resonance with a rather low maximum (and in different positions), while the data of Yarnell[YARNELL53A] and Freier[FREIER54A] showed much higher values. They could not, however, reveal the position of the maximum of the S-function. Yarnell published one total cross-section point only. Otherwise he gave $d\sigma/d\Omega$-data in graphic form. We integrated these data for $E \leq 1.5$ MeV and the total cross-sections are shown in Figure 10. Kliucharev published only the cross-section value at the maximum of the resonance[KLIUCHAREV56A]. Stewart's data[STEWART60A] covered the region of very high bombarding energies only, and did not help in resolving the problems with the position of the resonance. The new measurements of Möller et al.[MOELLER80A] and of Krauss et al.[KRAUSS87A] show a maximum at an energy close

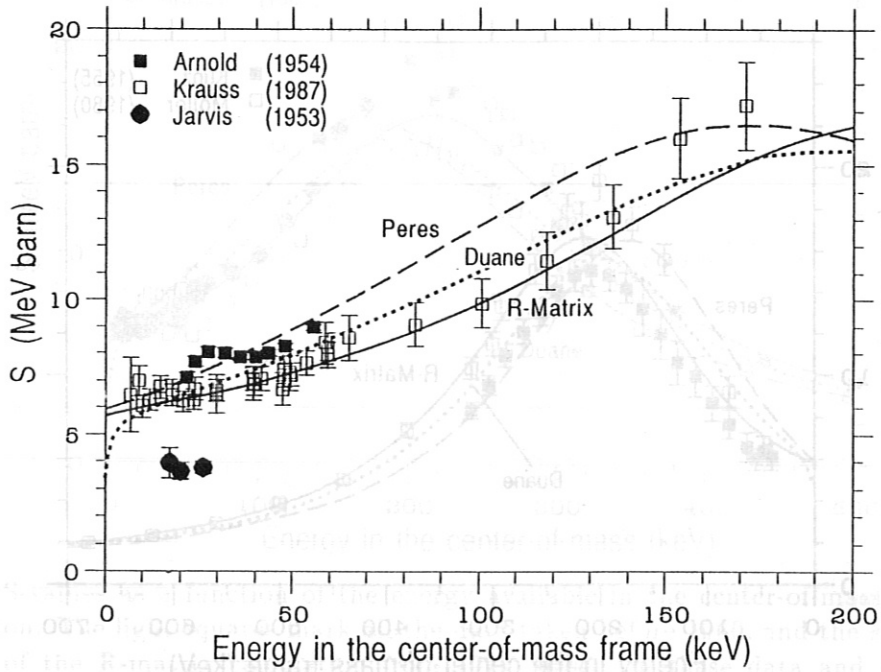

Figure 9: S-values as a function of the energy available in the center-of-mass frame for the D^3He-reaction. Jarvis's data are much too low and should not be used for any evaluation. Krauss' data were measured long after the R-matrix had been calculated, but they agree rather well with it, except for the two point at the highest energies.

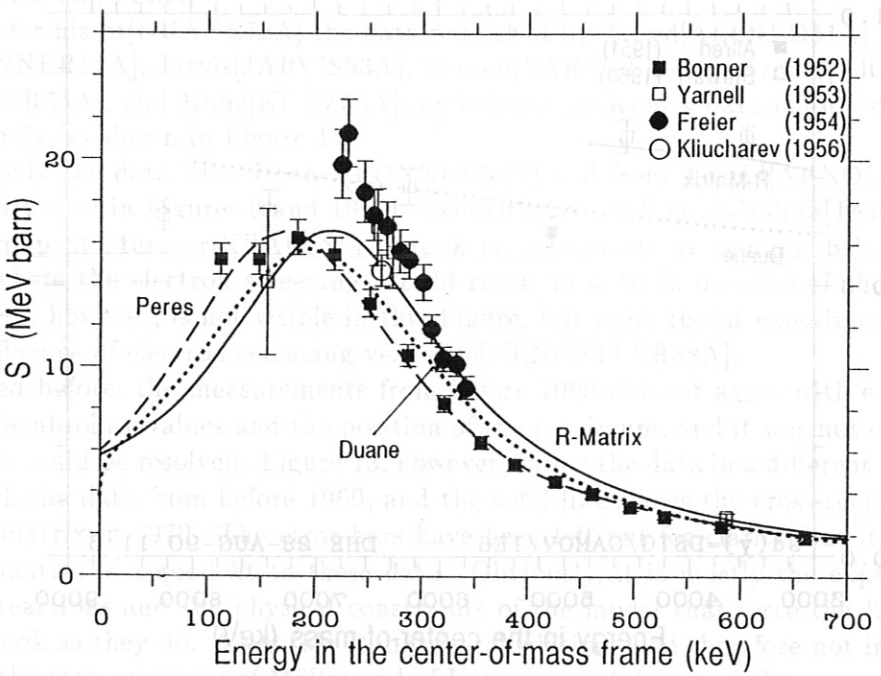

Figure 10: S-values as a function of the energy available in the center-of-mass frame for the D^3He-reaction. It was mainly the data set of Bonner that determined Peres's fit, as can be seen here.

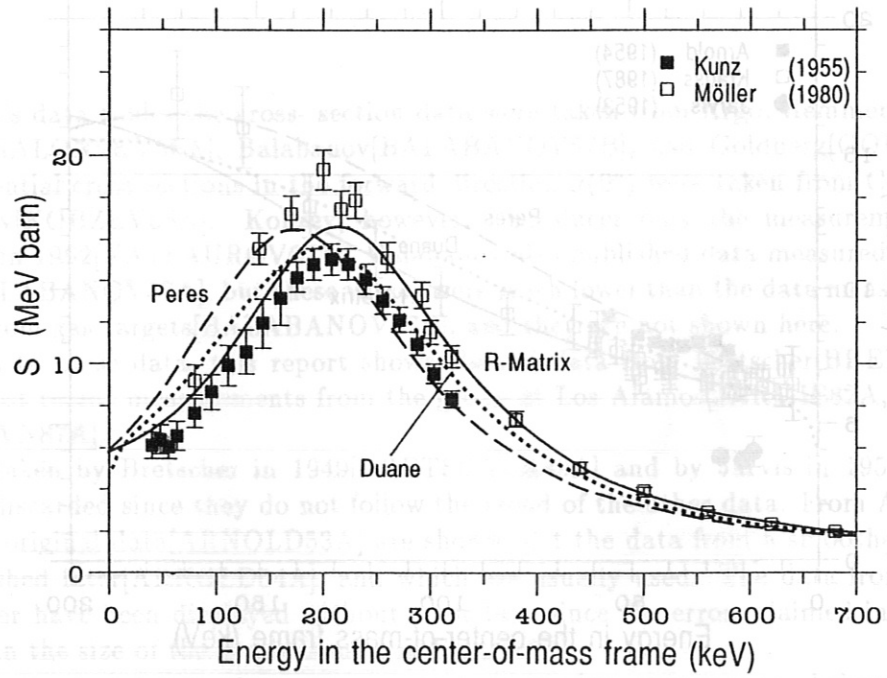

Figure 11: S-values as a function of the energy available in the center-of-mass frame for the D^3He-reaction. The data of Möller et al. were taken after the R-matrix calculation, but they agree rather well with these results, except in the region just below the resonance.

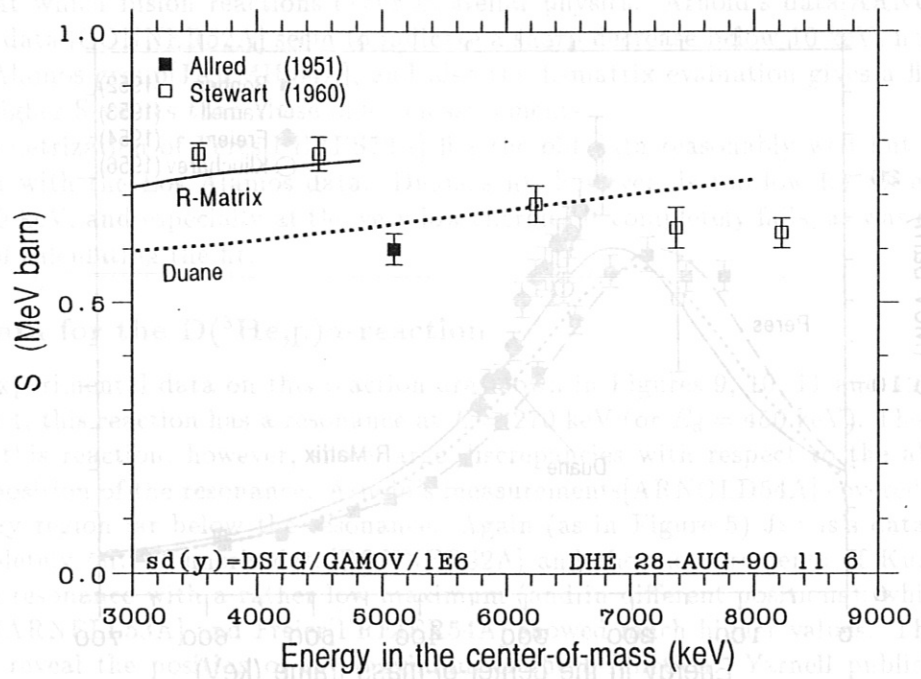

Figure 12: S-values as a function of the energy available in the center-of-mass frame for the D^3He-reaction at very high energy.

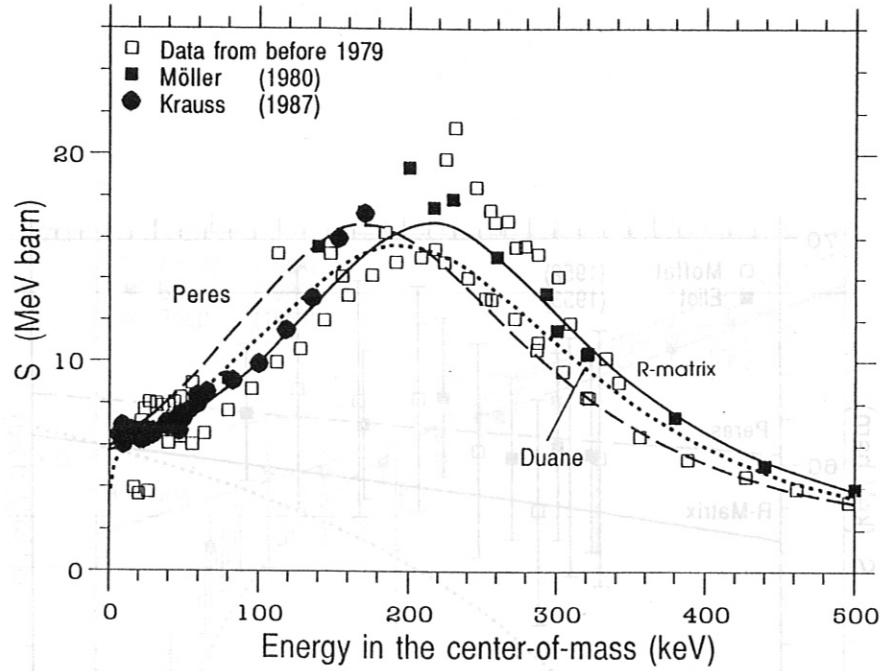

Figure 13: S-values as a function of the energy available in the center-of-mass frame for the D^3He-reaction. The light squares mark all the data taken before 1960, and the solid line shows the results of the R-matrix calculation from 1979, based on these data and data for other reactions. The dark symbols show the data taken later, which agree rather well with these R-matrix results, except for some discrepancy in the region of the resonance.

to that of Kunz, and their absolute values are between those of Bonner and Kunz and those of Arnold, Yarnell and Freier.
Duane used for his fit[DUANE72A] the data published by Allred[ALLRED51A], Bonner[BONNER52A], Jarvis[JARVIS53A], Yarnell[YARNELL53A], Arnold[ARNOLD54A], Freier[FREIER54A], and Kunz[KUNZ55A], and obviously Kunz's data mainly determined the cross-section fit, as shown in Figure 11.
Peres used only the data from Bonner[BONNER52A] and from Arnold[ARNOLD54A], as can be very clearly seen in Figures 9 and 10. He explicitly rejected Jarvis's data[JARVIS53A].
Only the group at Münster[KRAUSS87A] took measurements at energies below 11 keV (see Figure 9), where the electron screening should result in a 10 % increase of the cross-section. Such an effect, however, is not visible in this Figure, but more recent experiments at Münster show the influence of electron screening very nicely[ENGSTLER88A].
As mentioned before, the measurements from before 1960 did not agree with each other with respect to the absolute values and the position of the maximum, and it was not clear how these discrepancies could be resolved. Figure 13, however, shows the data in a different way. The light squares mark the data from before 1960, and the solid line shows the cross-sections calculated from the R-matrix in 1979. The error bars have been left out for clarity, but it does not look as if the R-matrix is a good fit to these data. Obviously, it is mostly the experimental data from other reactions and the physical constraints of the model that force the R-matrix cross-sections to look as they do. After this R-matrix calculation (and therefore not included in this evaluation) the measurements of Möller and of Krauss were taken, and they now agree very well with the R-matrix result (except just around the resonance). This shows very impressively that the R-matrix calculations really improve the cross-section evaluation (even if the experimental cross-section data are in disagreement) by also including data from other reactions.

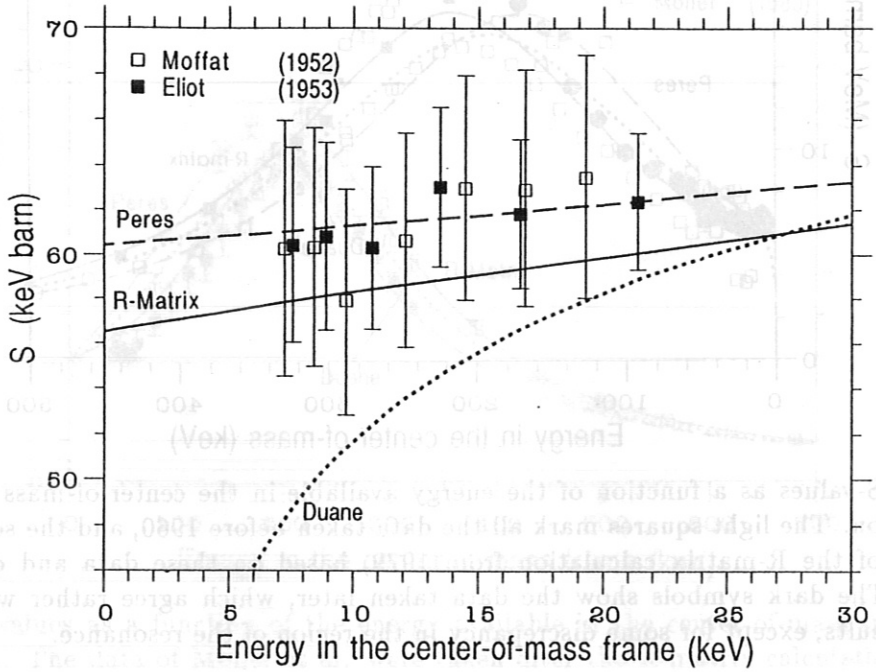

Figure 14: S-values as a function of the energy available in the center-of-mass frame for the D(d,p)T-reaction. Both data sets have appreciable error bars assigned to them, and they are higher than the R-matrix results.

3.4 Data for the D(d,p)T reaction

The experimental data on this reaction are shown in Figures 14, 15, 16, 17, 18, 19, and 20. As mentioned before, the non-resonant reactions show anisotropic emission of the reaction products in the center-of-mass frame even at low energies. These angular distributions, however, will not be treated here. Detailed measurements of the anisotropy have been made by several authors[MANNING42A, CHAGNON56A, FULLER57A, MILONE61A, RUBY63A], and this subject has been well summarized by Theus[THEUS66A]. More recent experiments have been made by, for example, Pospiech[POSPIECH75A], by the Münster group[KRAUSS87A] and the Los Alamos group[BROWN89A].
Duane used for his fit[DUANE72A] the data published by Blair[BLAIR48A], Moffat[MOFFAT52A], Davenport [DAVENPORT53A], Eliot [ELIOT53A], Arnold [ARNOLD54A], and Preston [PRESTON54A]. Peres's approximation formula[PERES79A] was calculated from the data of Moffat, Davenport, Arnold, Preston, McNeill [MCNEILL51A], Wenzel [WENZEL52A], Booth [BOOTH56A], Brolley[BROLLEY57A], and Schulte[SCHULTE72A]. Schulte, however, published Legendre coefficients only, and his data are not shown in this report. In addition to the data mentioned before, we show the data of Ganeev[GANEEV57A], von Engel[ENGEL61A], Krauss[KRAUSS87A], Jarmie and Brown[JARMIE85A, BROWN89A] and of Roth[ROTH90A]. Arnold's data in Figure 15 show a decline at the low energies and follow the trend of Duane's fit, but all the other data are more or less constant there (or show a flat decrease to lower energies) and do not follow Duane's fit. However, the data published by Arnold in 1954 are not the originally measured data but points from a smooth curve through these experimental data. Booth's data are much lower than all the other data and should not be used for a parametrization.

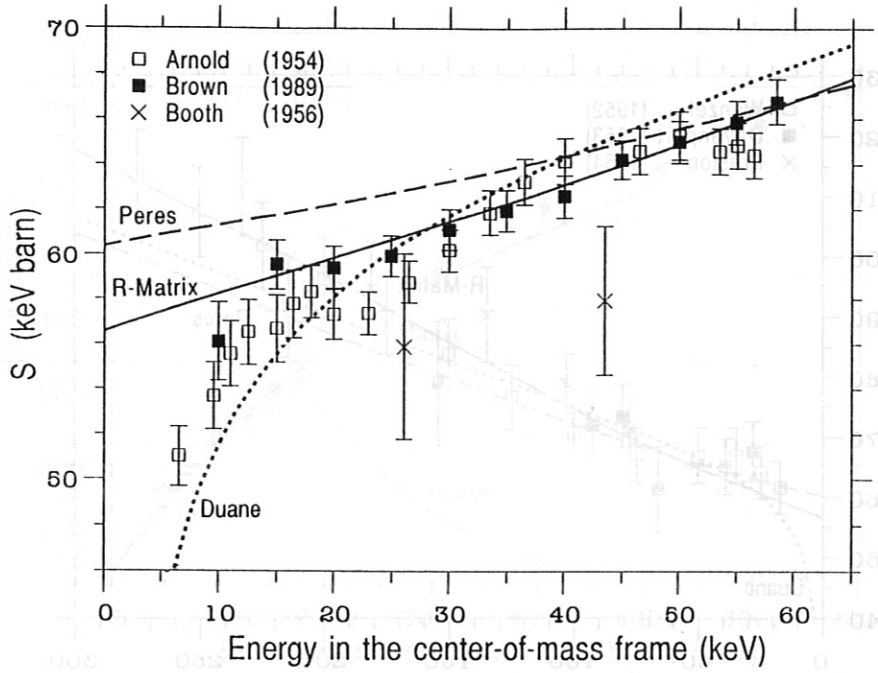

Figure 15: S-function of the D(d,p)T-reaction. Arnold's data (points of a smooth curve through the experimental data) decrease sharply towards low energies, unlike all other data sets. Booth's data are much lower than all the other data.

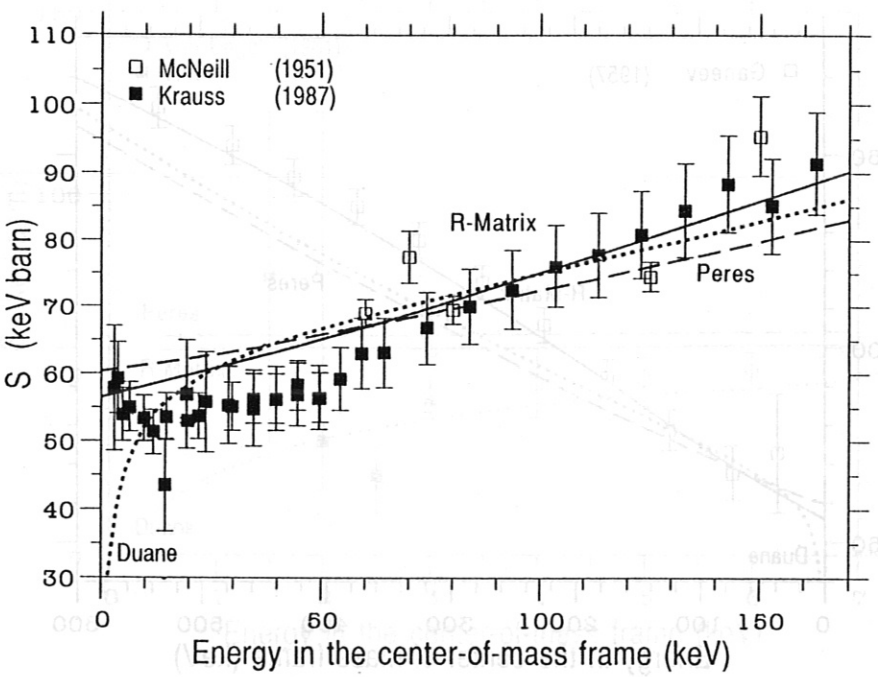

Figure 16: S-function of the D(d,p)T-reaction. Krauss et al. used two different accelerators for their measurements and the very low data point at about 15 keV is the lowest energy point of the high-energy accelerator experiments.

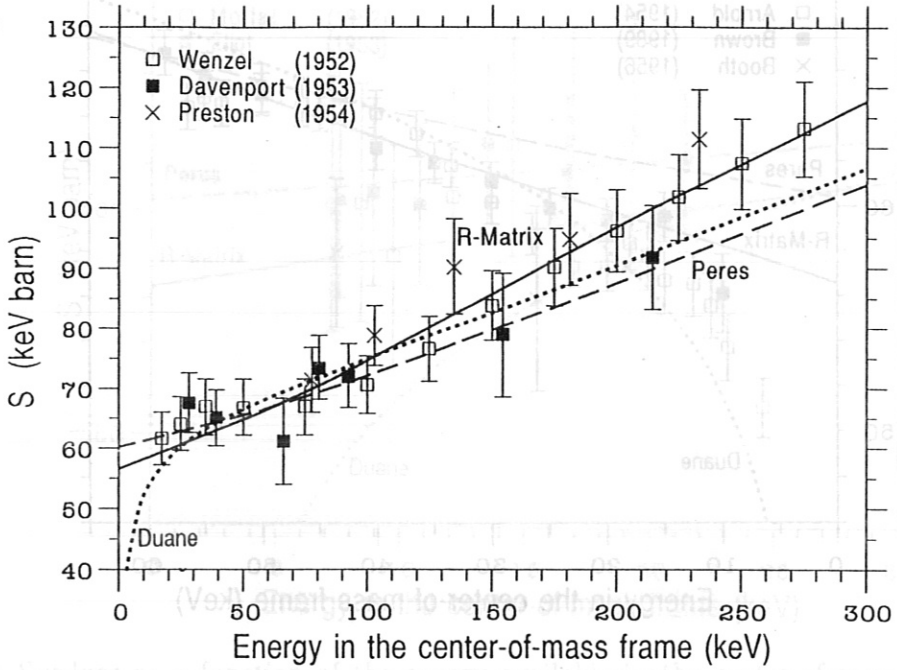

Figure 17: S-function of the D(d,p)T-reaction.

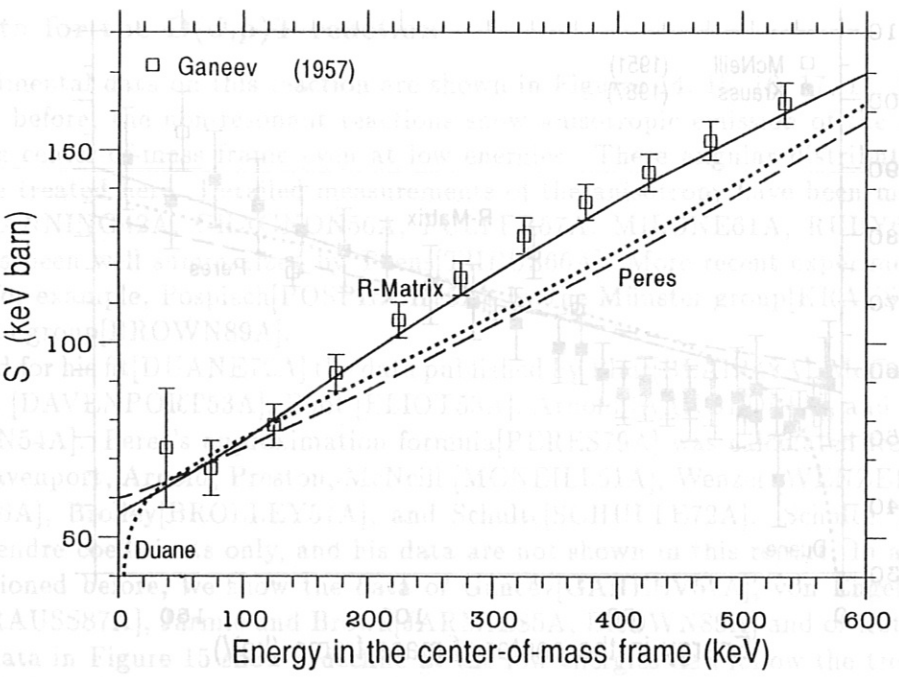

Figure 18: S-function of the D(d,p)T-reaction for higher energies. Ganeev's data agree well with the R-matrix values, but they are about 10 % above the old parametrizations.

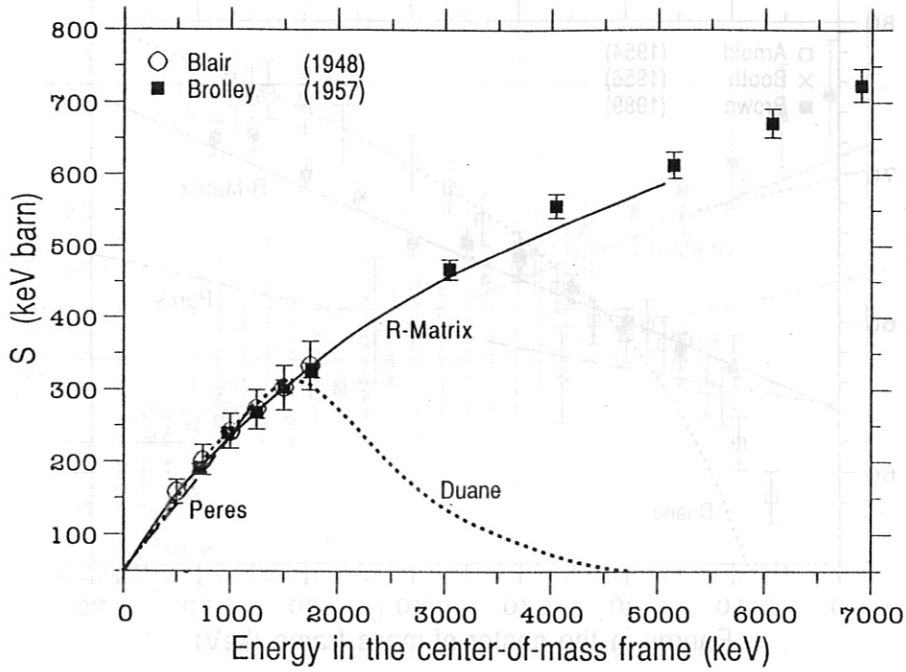

Figure 19: S-function of the D(d,p)T-reaction for MeV energies. Peres's fit is only valid up to 1 MeV. Duane's fit should work up to 10 MeV.

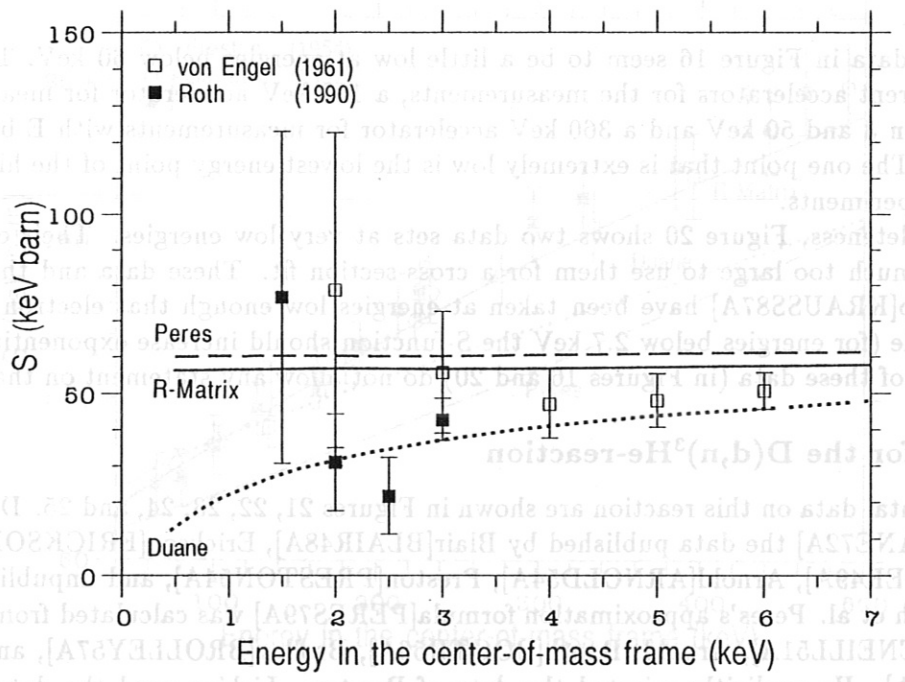

Figure 20: S-function of the D(d,p)T-reaction for the very low energy region. Roth's data were taken in the search for "cold fusion". The error bars for both data sets are very large, and these data should not be used for any fit, but rather for a comparison with the parametrizations.

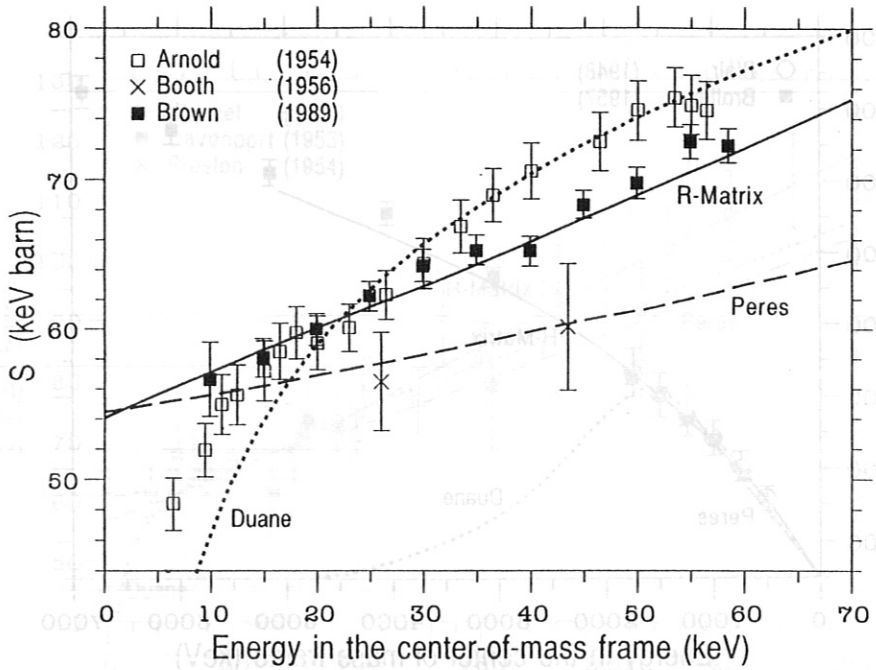

Figure 21: S-function of the D(d,n)^{3}He-reaction. As in the case of the D(d,p)T-reaction, Arnold's data decrease sharply towards low energies, unlike all other data sets, and again Booth's data are too low. Arnold's data have been corrected as described in the text.

The Münster data in Figure 16 seem to be a little low at energies below 60 keV. This group used two different accelerators for the measurements, a 100 keV accelerator for measurements with E between 3 and 50 keV and a 360 keV accelerator for measurements with E between 14 and 163 keV. The one point that is extremely low is the lowest energy point of the high-energy accelerator experiments.
Just for completeness, Figure 20 shows two data sets at very low energies. Their error bars, however, are much too large to use them for a cross-section fit. These data and those of the Münster group[KRAUSS87A] have been taken at energies low enough that electron screening could be visible (for energies below 2.7 keV the S-function should increase exponentially). But the error bars of these data (in Figures 16 and 20) do not allow any statement on that.

3.5 Data for the D(d,n)^{3}He-reaction

The experimental data on this reaction are shown in Figures 21, 22, 23, 24, and 25. Duane used for his fit[DUANE72A] the data published by Blair[BLAIR48A], Erickson[ERICKSON49A], Hunter[HUNTER49A], Arnold[ARNOLD54A], Preston[PRESTON54A], and unpublished data by R. K. Smith et al. Peres's approximation formula[PERES79A] was calculated from the data of McNeill[MCNEILL51A], Arnold, Booth[BOOTH56A], Brolley[BROLLEY57A], and Schulte [SCHULTE72A]. He explicitly rejected the data of Preston. Liskien used the data of Blair, McNeill, Hunter, Arnold, Preston, Booth, Brolley, Ganeev [GANEEV57A], Davidenko [DAVIDENKO57A], Goldberg[GOLDBERG60A], Thornton[THORNTON69A], and Schulte. Schulte published Legendre coefficients only, and his data are not shown in this report. Arnold's

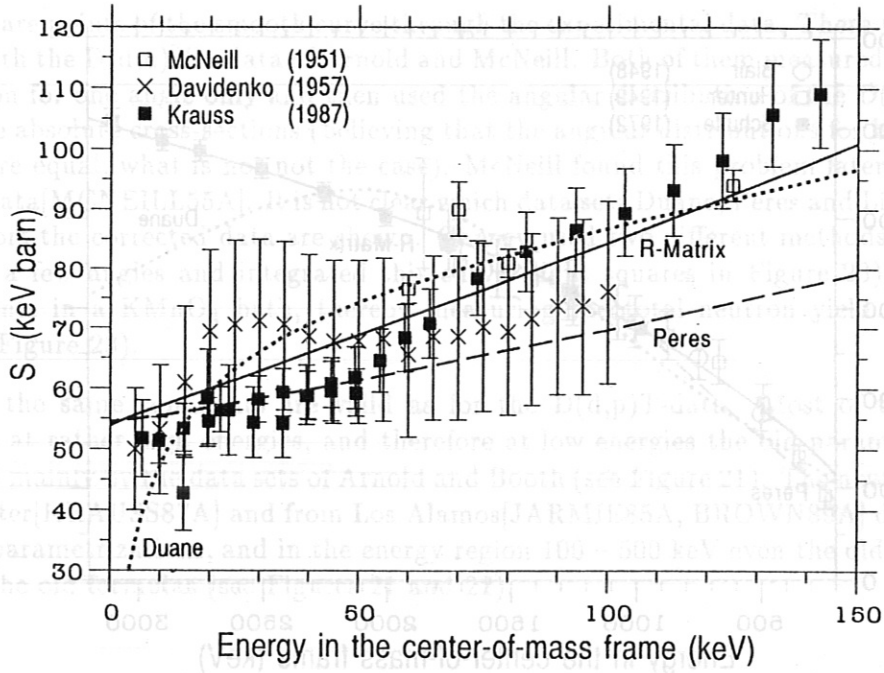

Figure 22: S-function of the D(d,n)^{3}He-reaction. McNeill's data have been corrected as described in the text.

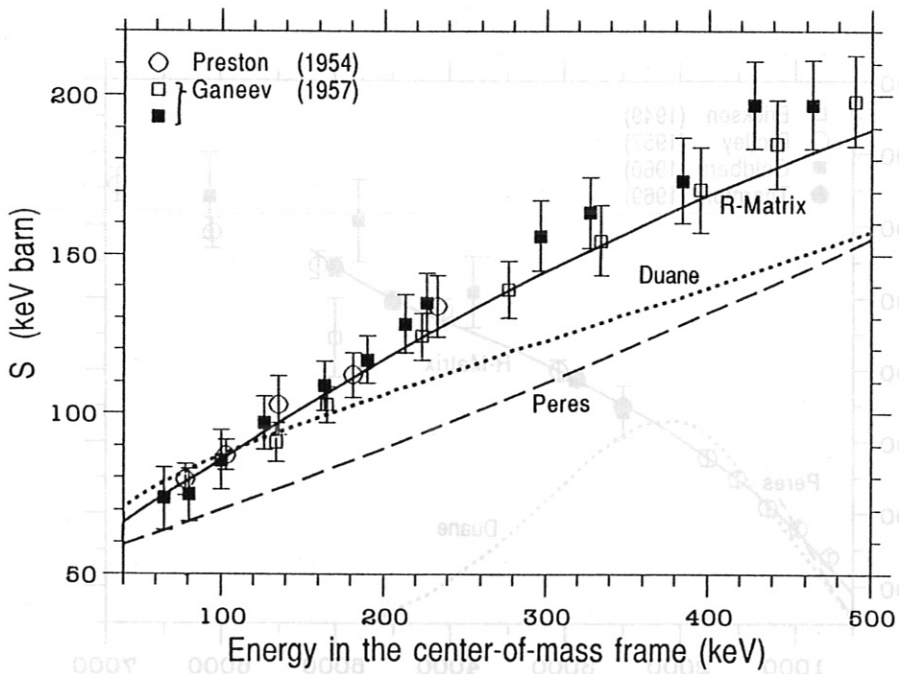

Figure 23: S-function of the D(d,n)^{3}He-reaction for higher energies. Ganeev used two different methods, numerical integration of differential cross-sections (light squares) and measurements in a $KMnO_4$ bath (black squares). Again in this energy region all experimental data are higher than the old parametrizations and agree with the R-matrix results.

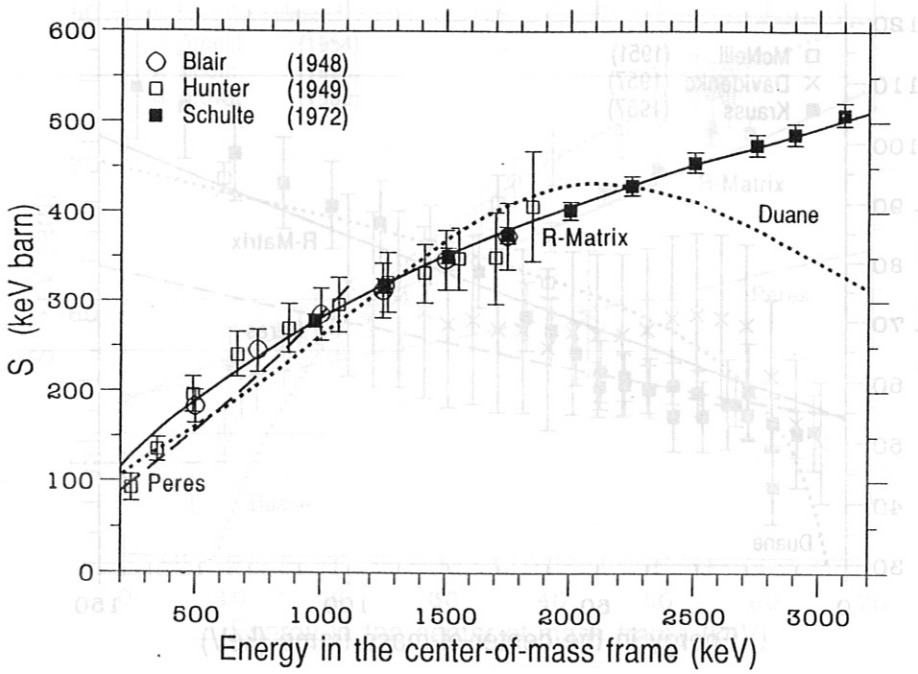

Figure 24: S-function of the D(d,n)^{3}He-reaction for MeV energies. Peres's fit is only valid up to 1 MeV. Duane's fit should work up to 10 MeV.

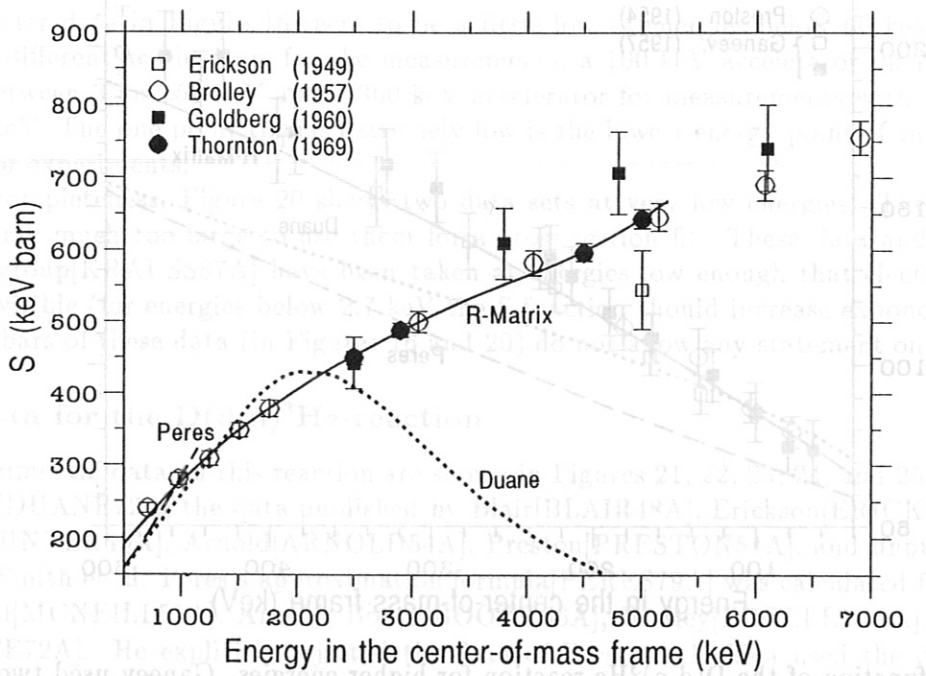

Figure 25: S-function of the D(d,n)^{3}He-reaction for MeV energies. Peres's fit is only valid up to 1 MeV. Duane's fit should work up to 10 MeV.

data again are points of the smooth curve through the experimental data. There was, however, a problem with the D(d,n)^{3}He-data of Arnold and McNeill. Both of them measured the differential cross-section for one angle only and then used the angular distribution of the D(d,p)T-reaction to calculate absolute cross-sections (believing that the angular distributions for both of the DD-reactions are equal, what is not not the case). McNeill found this problem later and published corrected data[MCNEILL55A]. It is not clear which data sets Duane, Peres and Liskien used, but in this report the corrected data are shown. Ganeev used two different methods: He measured $d\sigma/d\Omega$ for a few angles and integrated this curve (light squares in Figure 23), and he made measurements in a $KMnO_4$ bath, thereby measuring the total neutron yield directly (black squares in Figure 23).

In general the same comments are valid as for the D(d,p)T-data. Most of these data had been taken at rather high energies, and therefore at low energies the old parametrizations are determined mainly by the data sets of Arnold and Booth (see Figure 21). The new measurements from Münster[KRAUSS87A] and from Los Alamos[JARMIE85A, BROWN89A] do not fit either of the old parametrizations, and in the energy region 100 – 500 keV even the old measurements do not fit the old formulas (see Figures 21 and 22).

4 Cross-section parametrization

New parametrizations for the total fusion cross-section will now be given. For the reasons discussed earlier, however, we do not use the experimental data discussed before but cross-section values derived from R-matrix calculations.

4.1 Cross-sections from R-matrices

For the DT-reaction a final R-matrix has been published[HALE87A], and a table with cross-sections from this R-matrix was given in an internal memo[HALE86A]. These cross-sections are determined to within 2 % at energies of up to 1 MeV, with the error gradually increasing up to about 5 % at higher energies[HALEPERS]. Another memo[HALE79B] contains R-matrix cross-sections for the D^3He-reaction (status of July 1979) that are supposed to be correct to at least 10 %[HALEPERS]. For the DD-reactions, in contrast, the R-matrix calculations are still in progress but are approaching the final evaluation. The cross-sections, however, are already very stable, and they are supposed to be correct within 5 % for energies of up to 1 MeV, with the uncertainty increasing to about 10 % at the higher energies[HALEPERS].

4.2 The new parametrization

The parametrization is being done with the following formula:

$$\sigma = \frac{S(E)}{E \cdot e^{(B_G/\sqrt{E})}}. \tag{20}$$

Here the penetrability factor as derived by Gamov has been used since this form can be handled more easily if one wants to calculate reactivities analytically[BAHCALL66A, MIKKELSEN89A]. The S-values calculated from the R-matrix cross-sections with equation 20 were fitted with a Padé-polynomial:

$$S(E) = \frac{A1 + E \cdot (A2 + E \cdot (A3 + E \cdot (A4 + E \cdot A5)))}{1 + E \cdot (B1 + E \cdot (B2 + E \cdot (B3 + E \cdot B4)))}. \tag{21}$$

For the DT- and the DD-reactions these numerical fits were calculated with the "*nonlinear fit*" procedure of the LOCUS data-base system[MURPHY88A]. The data for the D^3He-reaction were evaluated later and this fit was done with the SAS program package[SAS]. The aim was to achieve a maximum deviation of the fit formula from the input data of less than 3 %, and fits with different numbers of parameters were made for all reactions to reach this goal with as few parameters as possible.

The results of the fit are given in Table 3 together with the Gamov constant B_G for each reaction. With E in keV the fusion cross-section is given in units of millibarn (1 millibarn = 10^{-27} m^{-2}). The two bottom lines of Table 3 show the energy range in which the approximation formulas 20 and 21 are valid, and also the maximum deviation of the approximation formula from the original R-matrix cross-sections.

For the non-resonant DD-reactions a single set of parameters was found which describes the data over the whole energy range sufficiently well. Figure 26 shows for both reactions the comparison of the new fit formula with the original R-matrix data.

The situation is different for the resonant reactions, where it was not possible to cover the whole energy range with a single fit. Here two fits for each reaction had to be calculated, which are

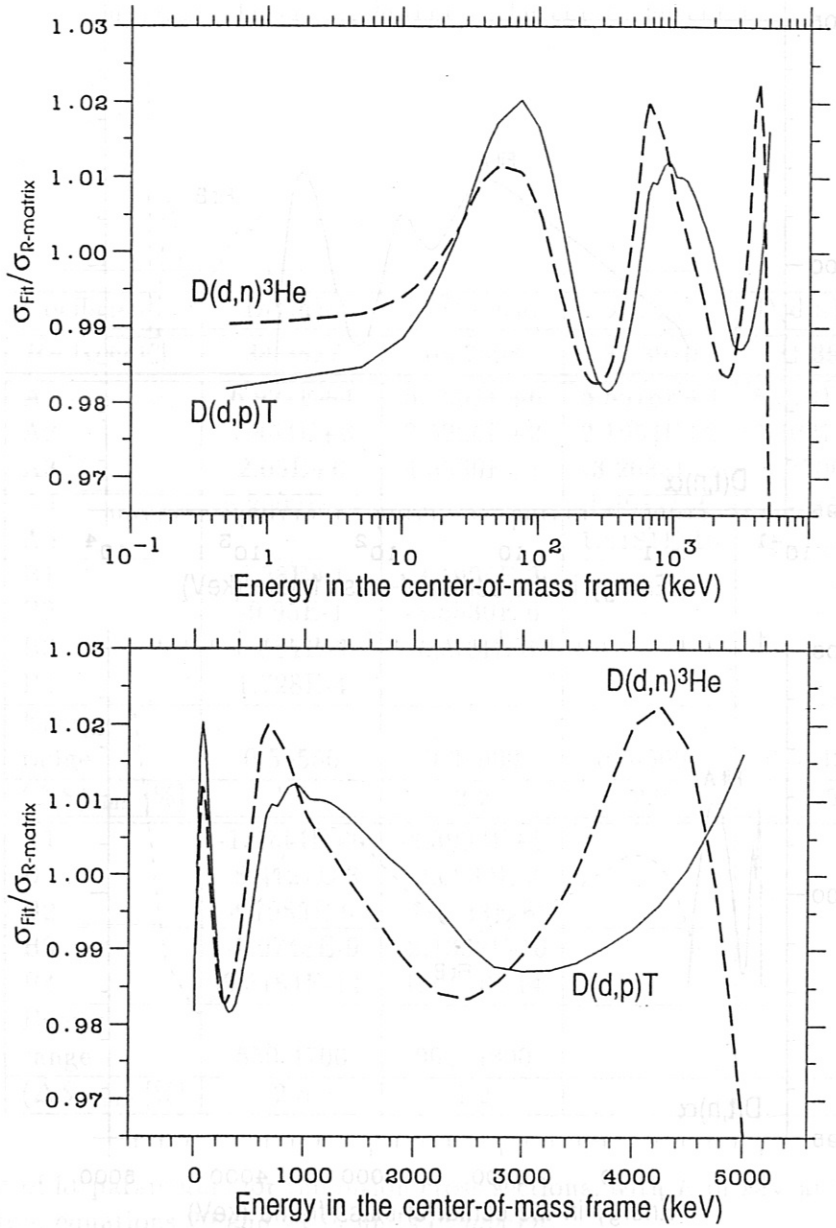

Figure 26: The cross-section for the non-resonant reactions calculated from our approximation formula divided by the original values from the R-matrix evaluation. For the proton branch the fit deviates less than 2.0 % from the input data for all energies, while for the neutron branch the deviation is less than 2.5 % for energies smaller than 4900 keV. Figure **(a)** shows this comparison on a logarithmic energy scale, while **(b)** has a linear energy axis.

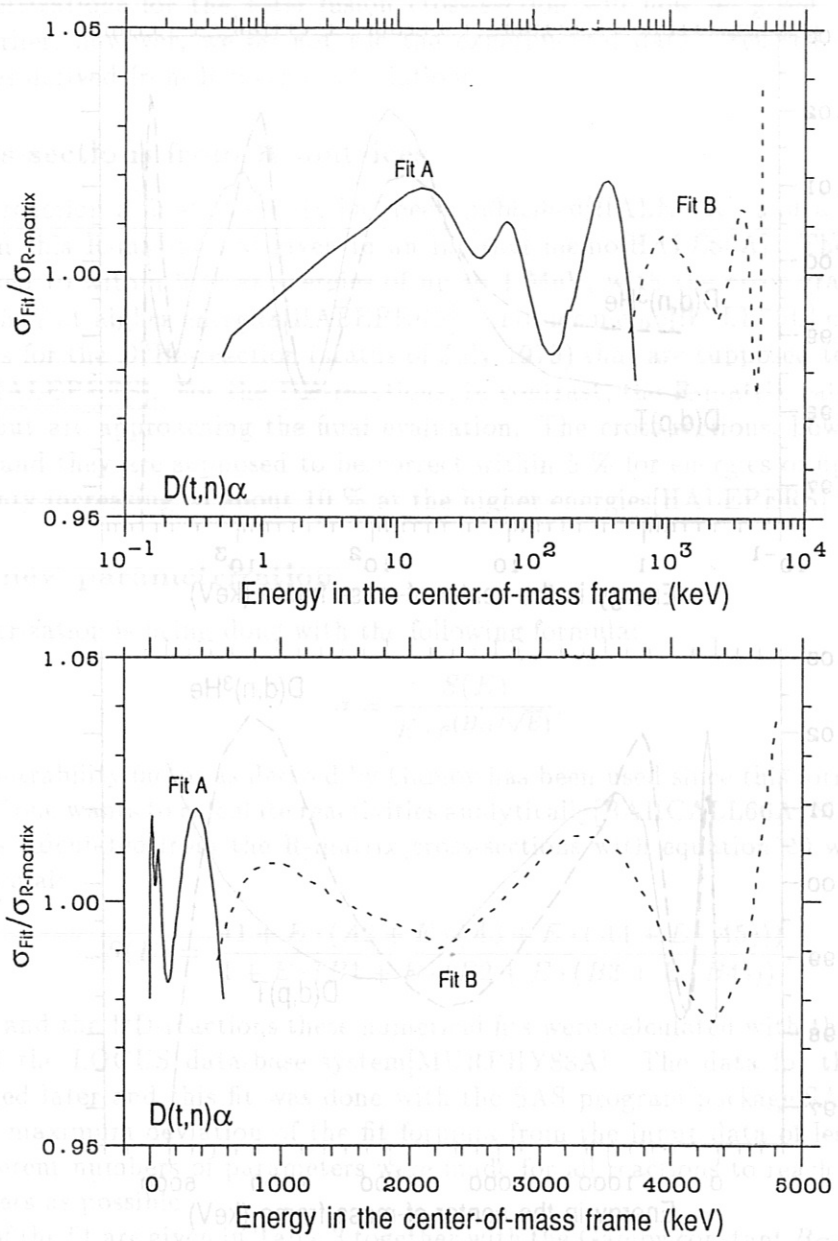

Figure 27: Comparison of the approximation formula for the D(T,n)α-reaction with the R-matrix data used for the fit. "Fit A" shows the comparison for the low-energy formula, while "Fit B" shows the high-energy formula. Again **(a)** uses a logarithmic energy axis, while **(b)** shows the comparison on a linear scale.

Coefficient	D(t,n)α	D(^{3}He,n)α	D(d,p)T	D(d,n)^{3}He
B_G $[\sqrt{keV}]$	34.3827	68.7508	31.3970	31.3970
A1	6.927E+4	5.7501E+6	5.5576E+4	5.3701E+4
A2	7.454E+8	2.5226E+3	2.1054E+2	3.3027E+2
A3	2.05E+6	4.5566E+1	-3.2638E-2	-1.2706E-1
A4	5.2002E+4	–	1.4987E-6	2.9327E-5
A5	–	–	1.8181E-10	-2.5151E-9
B1	6.38E+1	-3.1995E-3	–	–
B2	-9.95E-1	-8.5530E-6	–	–
B3	6.981E-5	5.9014E-8	–	–
B4	1.728E-4	–	–	–
Energy range	0.5–550	0.3–900	0.5-5000	0.5–4900
$(\Delta S)_{max}$ [%]	1.9	2.2	2.0	2.5
A1	-1.4714E+6	-8.3993E+5		
B1	-8.4127E-3	-2.6830E-3		
B2	4.7983E-6	1.1633E-6		
B3	-1.0748E-9	-2.1332E-10		
B4	8.5184E-14	1.4250E-14		
Energy range	550-4700	900–4800		
$(\Delta S)_{max}$ [%]	2.5	1.2		

Table 3: List of fit parameters for the fusion cross-sections, with E in keV and the cross-section calculated from equations 20 and 21 in units of *mbarn*.

E [keV]	D(t,n)α [$mbarn$]	D(^{3}He,n)α [$mbarn$]	D(d,p)T [$mbarn$]	D(d,n)^{3}He [$mbarn$]
3	9.808E-3	1.119E-11	2.513E-4	2.445E-4
4	1.073E-1	1.718E-9	2.146E-3	2.093E-3
5	5.383E-1	5.199E-8	9.038E-3	8.834E-3
6	1.749E+0	6.336E-7	2.569E-2	2.517E-2
7	4.335E+0	4.373E-6	5.720E-2	5.616E-2
8	8.968E+0	2.058E-5	1.081E-1	1.064E-1
9	1.632E+1	7.374E-5	1.820E-1	1.794E-1
10	2.702E+1	2.160E-4	2.812E-1	2.779E-1
12	6.065E+1	1.206E-3	5.607E-1	5.563E-1
15	1.479E+2	7.944E-3	1.180E+0	1.178E+0
20	4.077E+2	6.568E-2	2.670E+0	2.691E+0
30	1.381E+3	7.704E-1	6.681E+0	6.857E+0
40	2.817E+3	3.266E+0	1.116E+1	1.165E+1
50	4.219E+3	8.688E+0	1.557E+1	1.649E+1
60	4.984E+3	1.788E+1	1.971E+1	2.115E+1
70	4.987E+3	3.144E+1	2.351E+1	2.554E+1
80	4.545E+3	4.978E+1	2.698E+1	2.964E+1
100	3.427E+3	1.021E+2	3.304E+1	3.701E+1
120	2.576E+3	1.768E+2	3.812E+1	4.343E+1
140	2.004E+3	2.740E+2	4.245E+1	4.904E+1
150	1.792E+3	3.303E+2	4.438E+1	5.160E+1
200	1.138E+3	6.378E+2	5.234E+1	6.239E+1
250	8.135E+2	8.122E+2	5.831E+1	7.071E+1
300	6.234E+2	7.731E+2	6.302E+1	7.732E+1
400	4.126E+2	5.304E+2	7.005E+1	8.702E+1

Table 4: Cross-sections for all the reactions as a function of the energy in the center-of-mass frame. These values were calculated from eq. 20 and 21 with the parameters from Table 3.

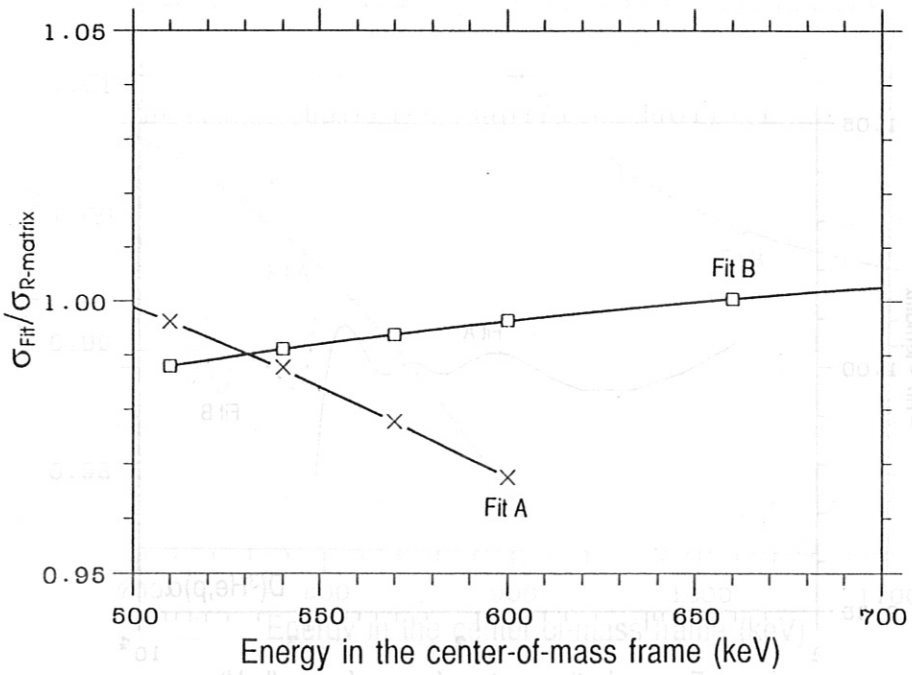

Figure 28: Region of the transition between the two approximation formulas for the D(T,n)α-reaction. The change of the formulas should be made somewhere between 500 and 600 keV.

also shown in Table 3 with their respective validity ranges. The formulas for the low-energy region (which covers the important region of the resonances) are marked as "fit A" in Figures 27 and 29, while "fit B" is the formula for the high-energy region. Figures 28 and 30 show the transition region between the two formulas.
For most applications, however, fit A will be sufficient. Even for burnup calculations where tritons start with an energy of 1.08 MeV (E = 430 keV) and ^{3}He-ions start with 820 keV (E = 330 keV) this fit is valid for the whole energy range needed. Only for high-energy ion tails (as produced in D(^{3}He) Minority Heating ICRH experiments) might the high energy formula be necessary.
Table 4 lists for all the reactions cross-sections as a function of the energy in the center-of-mass frame. These values have been calculated with the parameters from table 3.
A part of these new parametrizations has already been presented at the 17th European Plasma Physics Conference in Amsterdam, June 1990[BOSCH90A]. The table published in these proceedings, however, contained some errors, and should be replaced by the table presented in this report.

4.3 Comparison with the old parametrizations

Figures 31, 32, 33, 34, 35, 36, and 37 show for comparison the ratio of the cross-section given by different approximation formulas to the cross-section from the R-matrix calculations. For the resonant reactions this comparison is only done for the "low-energy" range. The fits given in this paper were already shown in Figures 26,27, and 29 in detail. All of the Figures displayed here show very clearly the systematic deviation of Duane's approximation formula at low energies.

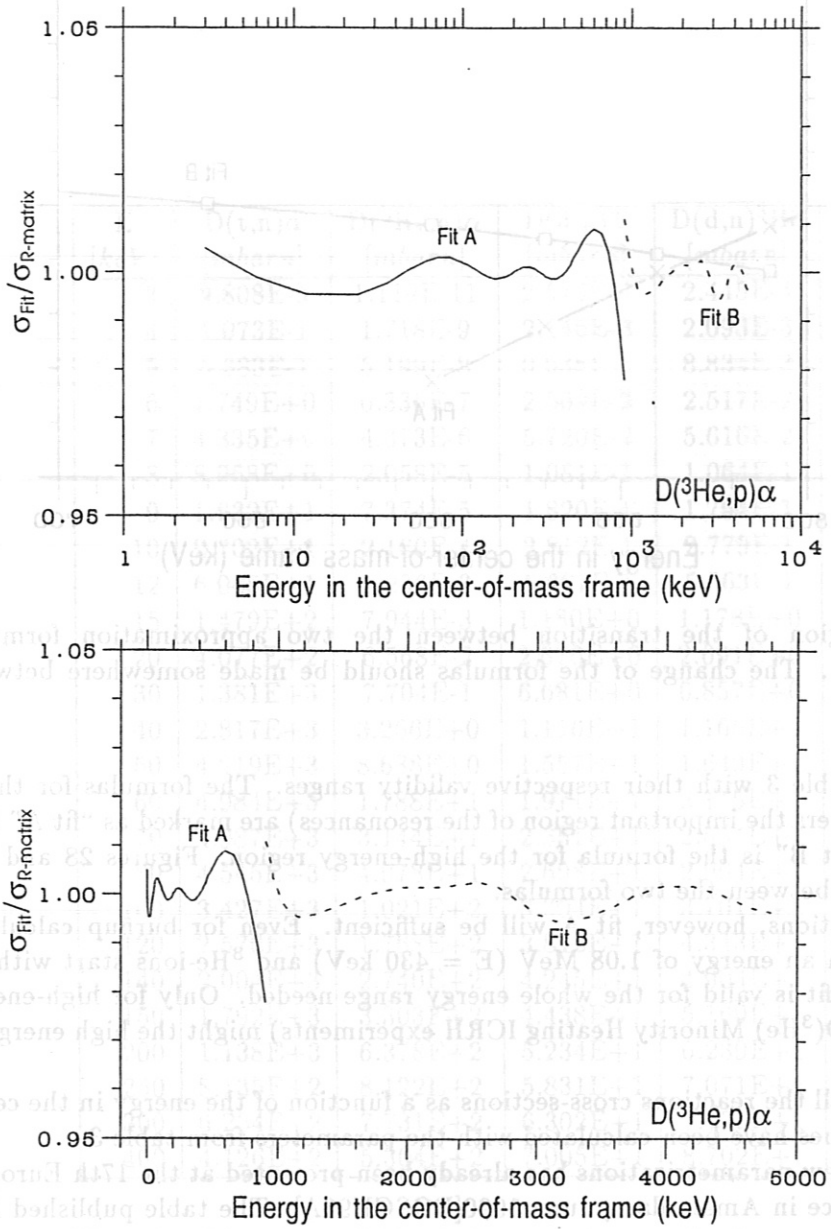

Figure 29: Comparison of the approximation formula for the D(^{3}He,p)α-reaction with the R-matrix data used for the fit. "Fit A" shows the comparison for the low-energy formula, while "Fit B" shows the high-energy formula. Again **(a)** uses a logarithmic energy axis, while **(b)** shows the comparison on a linear scale.

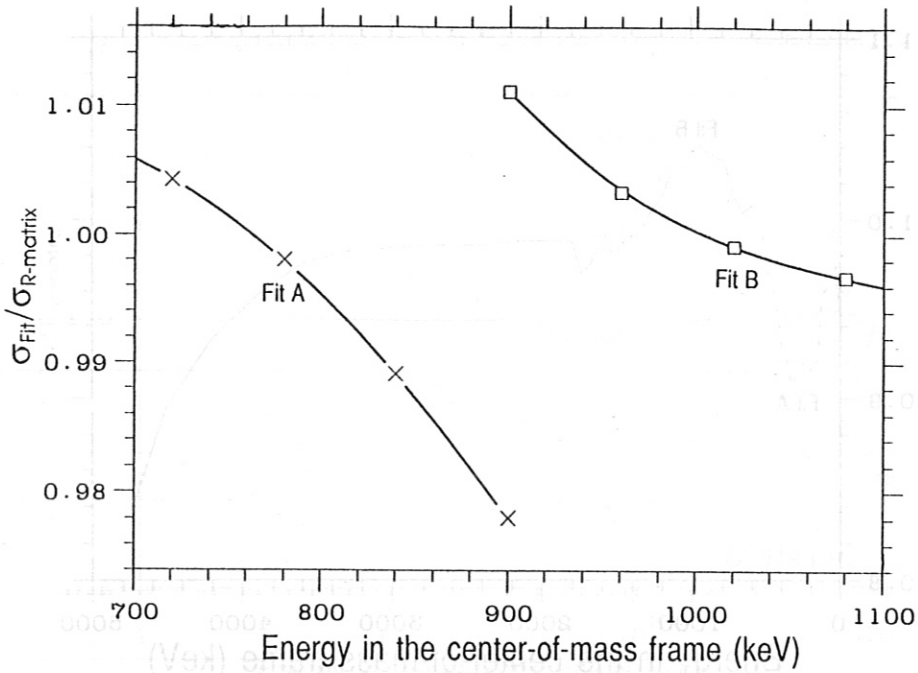

Figure 30: Transition of the two approximation formulas for the D(^{3}He,p)α-reaction. The transition energy of 900 keV should be carefully watched.

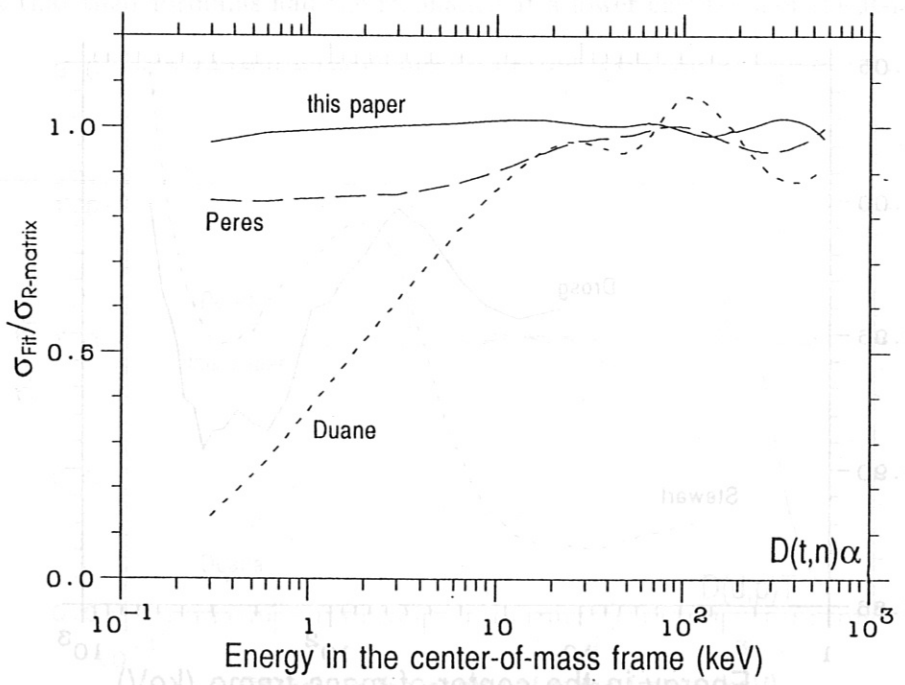

Figure 31: Comparison of the cross-sections calculated from the approximation formulas with the data from the R-matrix for the D(T,n)α-reaction. The solid line shows the fit A from Figure 27.

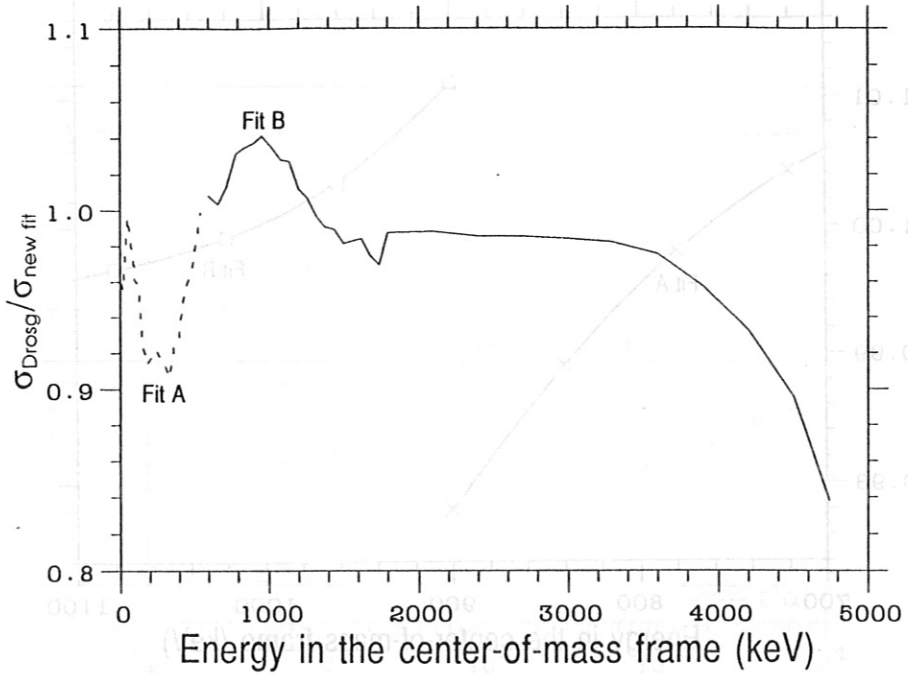

Figure 32: Comparison of the cross-sections from Drosg's spline fit and from Stewart's early R-matrix calculation with the new approximation formula presented in this report (i.e. fit A from Table 3).

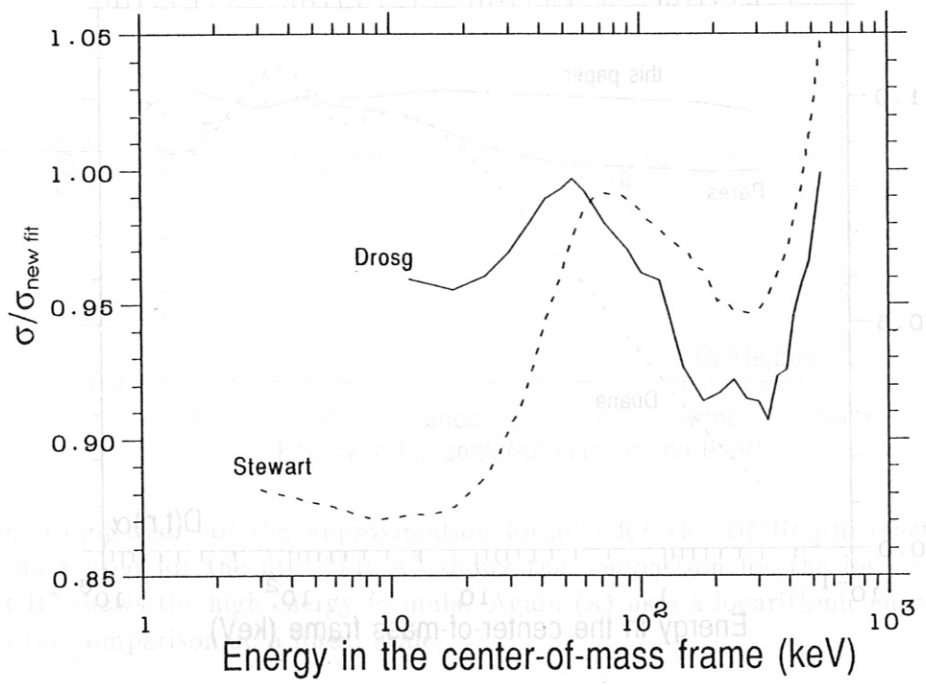

Figure 33: Comparison of the cross-sections from Drosg's spline fit with the new approximation formula presented in this report (see Table 3).

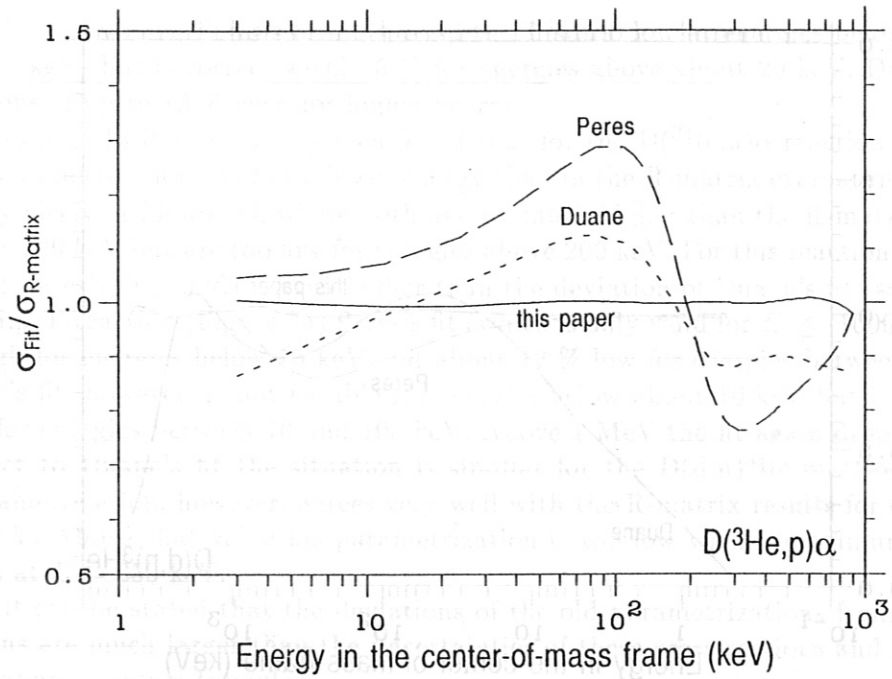

Figure 34: Comparison of the cross-sections calculated from the approximation formulas with the data from the R-matrix for the D(^{3}He,p)α-reaction. The solid line shows fit A from Figure 29. The steep variation of the cross-section ratio for Duane's and Peres's fit are a consequence of the fact that their formulas had the resonance at a lower energy than the R-matrix does.

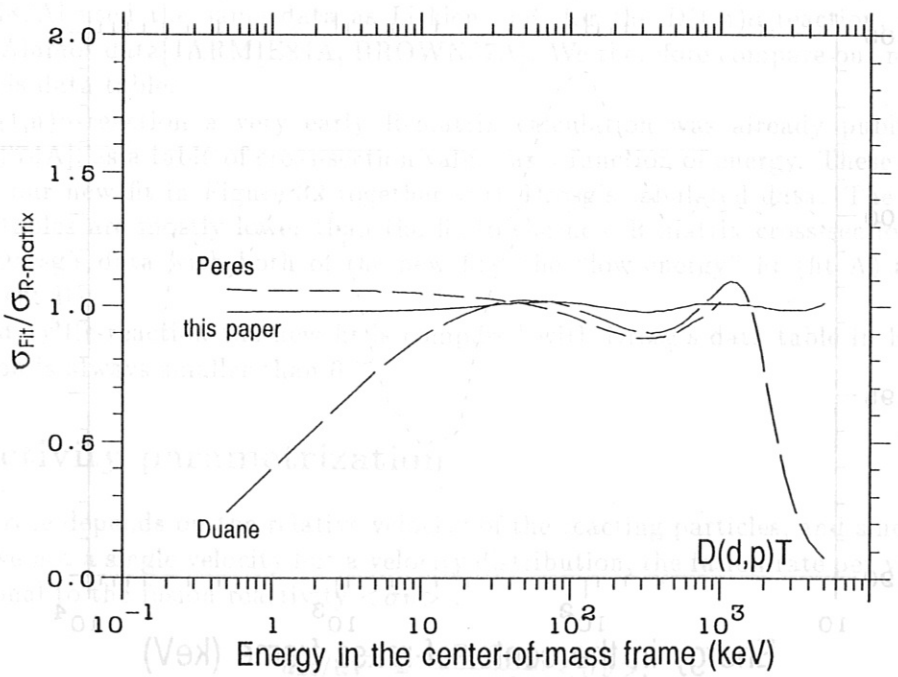

Figure 35: Comparison of the cross-sections calculated from the approximation formulas with the data from the R-matrix for the D(d,p)T-reaction. The solid line shows the fit from Figure 26.

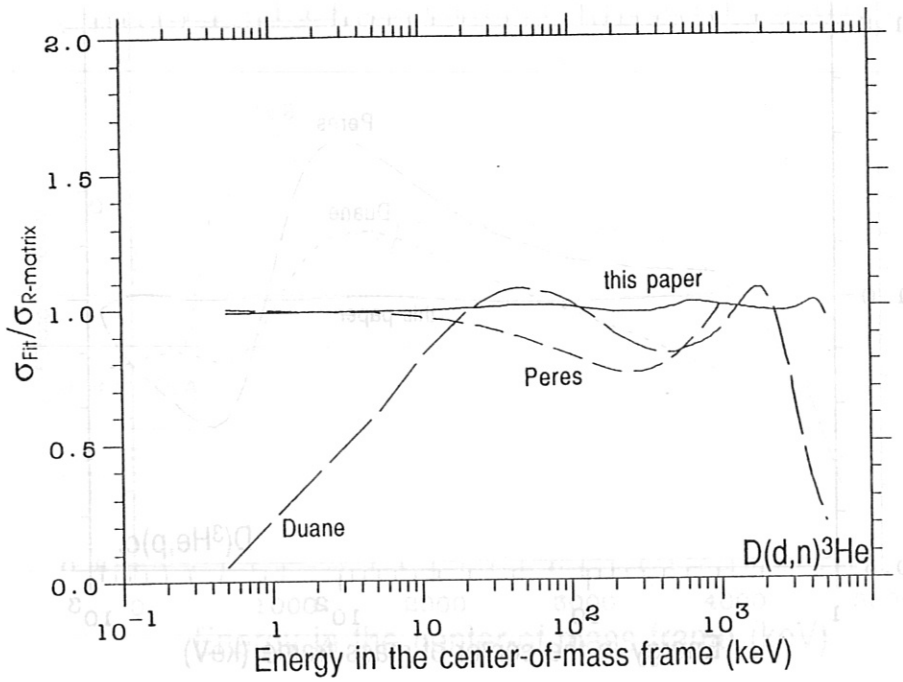

Figure 36: Comparison of the cross-sections calculated from the approximation formulas with the data from the R-matrix for the D(d,n)^{3}He-reaction. The solid line shows the fit from Figure 26.

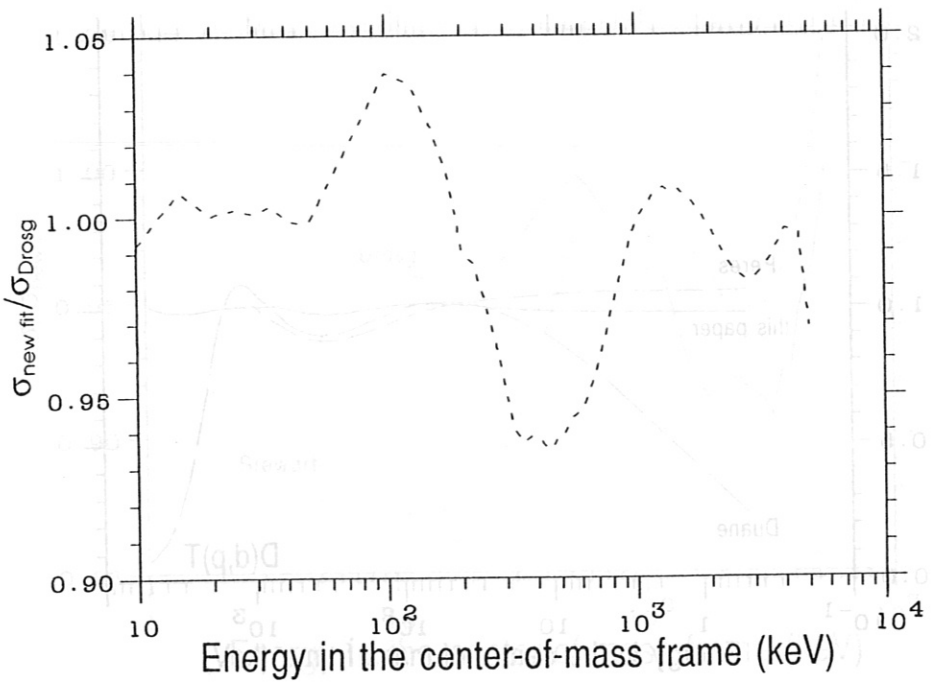

Figure 37: Comparison of the cross-sections calculated from the new approximation formulas with the data from Drosg et al.

For the D(T,n)α-reaction Peres's formula is up to 17 % too low at energies below about 5 keV (or $E_d \approx 8.3$ keV) but is correct within 5 % for energies above about 20 keV. Duane's formula has deviations of up to 13 % even for higher energies.
With Figures 9 to 13 it was already mentioned that for the D(^{3}He,n)α-reaction the maximum in the old parametrizations was at a lower energy than in the R-matrix evaluation, and this can be seen very nicely in Figure 34, where both fits are much higher than the R-matrix for energies below about 200 keV but are too low for energies above 200 keV. For this reaction the maximum deviation of Peres's fit (30 %) is even higher than the deviation of Duane's fit ($\approx$ 15 %).
For the D(d,p)T-reaction (Figure 35) Peres's fit (which is only valid for $E \leq 1000$ keV) is about 8 % too high for energies below 10 keV and about 12 % low for energies between 200 and 400 keV. Duane's fit, however, is not useable for energies below about 10 keV but is only up to 12 % too low for energies between 10 and 100 keV. Above 1 MeV the fit again drops very rapidly.
With respect to Duane's fit the situation is similiar for the D(d,n)^{3}He-reaction (Figure 36). Peres's parametrization, however, agrees very well with the R-matrix results for energies below about 10 keV. Above that value his parametrization is too low with a maximum deviation of about 25 % at $E = 250$ keV.
In general, it can be stated that the deviations of the old parametrizations from the R-matrix cross-sections are much larger than the uncertainties of these cross-sections and the deviations of the new approximation formulas.

4.4 Comparison of the new fit with existing data tables

For the neutron-producing reactions D(d,n)^{3}He and D(t,n)α, tables with data from a spline fit to the experimental data have also been published[LISKIEN73A, DROSG87A]. Drosg et al.[DROSG87A] used the same data as Liskien and, for the D(t,n)α-reaction, also the most recent Los Alamos data[JARMIE84A, BROWN87A]. We therefore compare our new fit formula only with his data table.
For the D(t,n)α-reaction a very early R-matrix calculation was already published in 1974 [STEWART74A], as a table of cross-section values as a function of energy. These data are compared with our new fit in Figure 32 together with Drosg's tabulated data. The cross-sections from both tables are mostly lower than the fit to the new R-matrix cross-sections. Figure 33 compares Drosg's data with both of the new fits, the "low energy" fit (fit A) and the "high energy" fit (fit B).
For the D(d,n)^{3}He-reaction the new fit is compared with Drosg's data table in Figure 37, and the deviation is always smaller than 6 %.

5 Reactivity parametrization

The fusion rate depends on the relative velocity of the reacting particles, and since in a plasma the ions have not a single velocity but a velocity distribution, the fusion rate per volume dR/dV is proportional to the fusion reactivity $<\sigma v>$:

$$dR/dV = \frac{n_i\, n_j}{1 + \delta_{ij}} \cdot <\sigma v>, \qquad (22)$$

n_i, n_j being the particle densities and $\delta_{ij} = \delta(i - j)$ the Kronecker symbol. If $f(\vec{v}_i)$ is the

T [keV]	E_0 [keV]	ΔE_0 [keV]
1	6.254	5.78
2	9.9	10.3
5	18.3	22.1
10	29.0	39.4
20	46.1	70.2

Table 5: Position and width of the Gamov peak as a function of the ion temperature for the DD-reactions.

velocity distribution of a particle, and g is the relative velocity ($\vec{g} = \vec{v}_i - \vec{v}_j$), one then gets

$$<\sigma v> = \int\int f(\vec{v}_i)\, f(\vec{v}_j)\, \sigma(|g|)\, |g|\, d\vec{v}_i\, d\vec{v}_j. \tag{23}$$

This is a six-fold integral, but in some cases it can be reduced to a simpler integral by symmetry considerations[CORE87B], and also approximation formulas for this integral have been derived analytically, for Maxwellian ion energy distributions [BAHCALL66A] as well as for beam-target reactivities[CORE87B, MIKKELSEN89A]. These formulas, however, are not very handy, and for most applications not accurate enough. For the D(T,n)α- and the D(^{3}He,p)α-reaction also a full calculation of the Fokker-Planck-equation has been used to evaluate the reactivities[FUTCH72A]. Such numerical caluclations are also necessary to evaluate the influence of fast ion tails from neutral beam heating and ICRH that can increase the fusion reactivity significantly[NIIKURA90A].
If one looks at the integrand in equation 23, it becomes obvious that fusion reactions occur only for a very limited energy range. The ion energy distribution usually decays very rapidly towards higher energies (for Maxwellian plasmas like $\exp(-E/kT)$), while the cross-section increases strongly with energy. Therefore the product of both factors has a relatively sharp maximum. If one approximates (very crudely) the cross-section as $\sigma \propto 1/E \cdot exp(-b/E^{1/2})$ (i. e. a constant S-function), it can be shown[CLAYTON74A] that this maximum occurs at an energy E_0. with

$$E_0 = 6.254 \cdot (Z_1^2 Z_2^2 A)^{1/3} \cdot T^{2/3} \tag{24}$$

when the ion temperature T and E_0 are measured in keV. A is the reduced mass of the system in amu. The full width of this so called "Gamov peak" is

$$\Delta E_0 = 5.78 \cdot (Z_1^2 Z_2^2 A)^{1/6} \cdot T^{5/6} \tag{25}$$

again with ΔE_0 and T in keV. This means, the cross-sections are important only in the energy range $E_0 - 1/2 \cdot \Delta E \longrightarrow E_0 + 1/2 \cdot \Delta E$. For all the other energies the contribution to the reactivity integral is too small to have an effect.
For the DD-reactions (where $Z_1 = Z_2 = A = 1$) the S-functions are rather flat, and this equations can be applied. Table 5 shows E_0 and ΔE_0 as a function of the ion temperature, and it can be seen that the Gamov-peak occurs always at energies much higher than the ion temperature. For the resonant reactions this simple equation should not be used due to the strong energy dependence of the S-functions.

Coefficient	D(t,n)α	D(^{3}He,n)α	D(d,p)T	D(d,n)^{3}He
B_G $[\sqrt{keV}]$	34.3827	68.7508	31.3970	31.3970
$m_r c^2$ $[keV]$	1 124 656	1 124 572	937 814	937 814
C1	1.17302E-9	5.74129E-10	5.65718E-12	5.43360E-12
C2	1.51361E-2	4.15827E-3	3.41267E-3	5.85778E-3
C3	7.51886E-2	1.90541E-2	1.99167E-3	7.68222E-3
C4	4.60643E-3	2.45907E-4	0.0	0.0
C5	1.35000E-2	4.26442E-4	1.05060E-5	-2.96400E-6
C6	-1.06750E-4	0.0	0.0	0.0
C7	1.36600E-5	7.13700E-6	0.0	0.0
$(\Delta<\sigma v>)_{max}$ [%]	0.25	0.5	0.35	0.3

Table 6: List of the fit parameters for the fusion reactivity in Maxwellian plasmas. With T_i in keV the reactivity is in cm^3/s. All the fits are valid for ion temperatures 0.2 keV $\leq$ T_i $\leq$ 100 keV.

5.1 Status of the parametrizations

At the very beginning of fusion research graphical[TUCK54A, TUCK61A] and tabulated reactivity data[GREENE67A] for thermal plasmas were published. These reactivities had been numerically integrated from cross-section data in the early reviews[JARMIE56A]. As the data base of the cross-sections grew, quite a few reports on reactivities were published[MCNALLY79A], often as internal reports only, and we apologize for omissions.
Later analytic expressions for thermal reactivities were presented by, among others, Brueckner and Jorna[BRUECKNER74A], Peres[PERES79A], Hively et al.[HIVELY77A, HIVELY83A], and Brunelli[BRUNELLI80A]. The latter three parametrizations, which have been widely used, are based on Duane's[DUANE72A] cross-section formulas.
Johner calculated a very crude (monomial) approximation for the D(t,n)α-reaction based on Peres's cross-section formula[JOHNER87A].
D. Slaughter[SLAUGHTER83A] calculated reactivities for a variety of ion energy distributions and also parametrized his results.
As all these reactivity evaluations, however, use the old cross-section parametrizations, which do not represent the cross-sections well enough, as we have seen before, it seems necessary to calculate new reactivities, on the basis of the cross-sections calculated from the final R-matrices. This will be done for the case of thermal plasmas (i.e. Maxwellian ion energy distributions) in the next section.
Recently preliminary R-matrix results for the D(t,n)α-reaction were used to derive a new cross-section parametrization and a parametrization of thermal reactivities[SADLER87B]. This is very similiar to what we did here, but we used the final R-matrix, and we used the cross-section values from the R-matrix fit directly, while Sadler had to calculate the cross-sections again from the published R-matrix parameters.

5.2 The new parametrization

G. M. Hale calculated thermal reactivities on the basis of the new R-matrix cross-sections[HALE79B, HALE86A, HALEPERS], and we used these reactivities to calculate a new parametrization. For

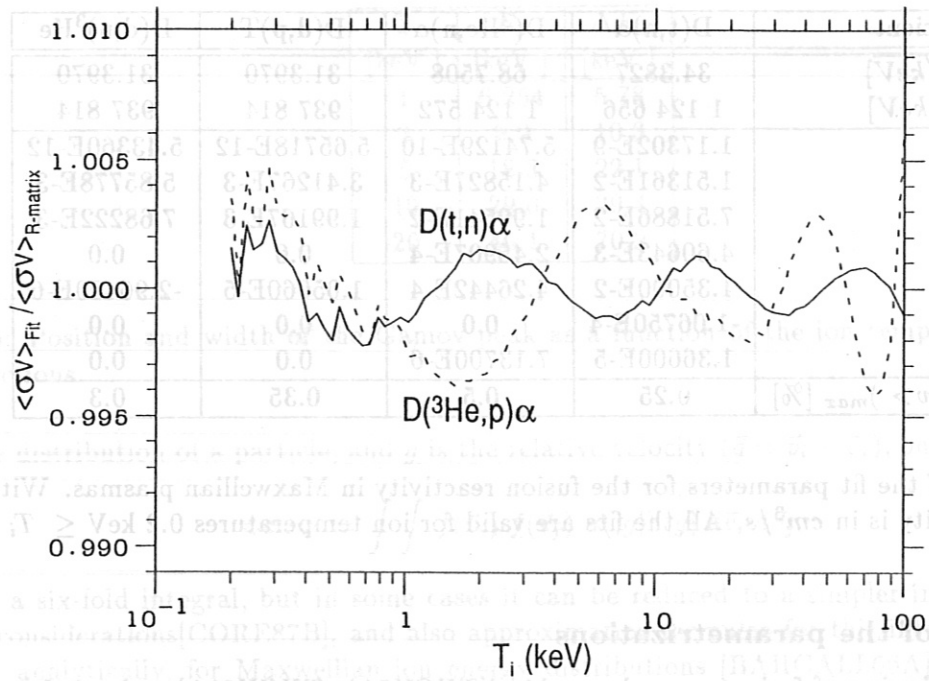

Figure 38: Comparison of the thermal reactivities calculated with the fit presented in this paper and the reactivities directly calculated from the R-matrix cross-sections for the resonant reactions.

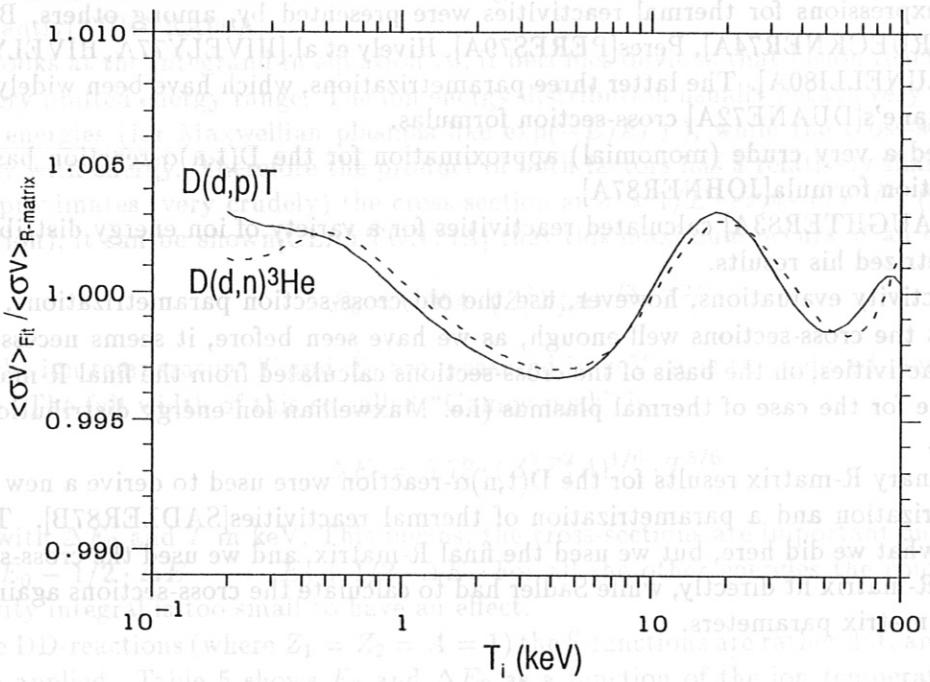

Figure 39: Comparison of the new fit formula with the input data for the non-resonant fusion reactions.

T_i $[keV]$	D(t,n)α $[cm^3/s]$	D(^{3}He,n)α $[cm^3/s]$	D(d,p)T $[cm^3/s]$	D(d,n)^{3}He $[cm^3/s]$
0.2	1.254E-26	1.461E-35	4.640E-28	4.482E-28
0.3	7.292E-25	1.065E-32	2.071E-26	2.004E-26
0.4	9.344E-24	6.720E-31	2.237E-25	2.168E-25
0.5	5.697E-23	1.273E-29	1.204E-24	1.169E-24
0.6	2.253E-22	1.194E-28	4.321E-24	4.200E-24
0.7	6.740E-22	7.114E-28	1.193E-23	1.162E-23
0.8	1.662E-21	3.094E-27	2.751E-23	2.681E-23
1.0	6.857E-21	3.109E-26	1.017E-22	9.933E-23
1.3	2.546E-20	2.626E-25	3.387E-22	3.319E-22
1.5	6.923E-20	1.331E-24	8.431E-22	8.284E-22
1.8	1.539E-19	4.850E-24	1.739E-21	1.713E-21
2.0	2.977E-19	1.407E-23	3.150E-21	3.110E-21
2.5	8.425E-19	7.482E-23	7.969E-21	7.905E-21
3.0	1.867E-18	2.668E-22	1.608E-20	1.602E-20
4.0	5.974E-18	1.695E-21	4.428E-20	4.447E-20
5.0	1.366E-17	6.297E-21	9.024E-20	9.128E-20
6.0	2.554E-17	1.713E-20	1.545E-19	1.573E-19
8.0	6.222E-17	7.380E-20	3.354E-19	3.457E-19
10.0	1.136E-16	2.094E-19	5.781E-19	6.023E-19
12.0	1.747E-16	4.661E-19	8.723E-19	9.175E-19
15.0	2.740E-16	1.171E-18	1.390E-18	1.481E-18
20.0	4.330E-16	3.512E-18	2.399E-18	2.603E-18
30.0	6.681E-16	1.392E-17	4.728E-18	5.271E-18
40.0	7.998E-16	3.201E-17	7.249E-18	8.235E-18
50.0	8.649E-16	5.528E-17	9.838E-18	1.133E-17

Table 7: Thermal reactivities for all the reactions as a function of the ion temperatur.

this parametrization we used the functional form proposed by A. Peres[PERES79A]:

$$<\sigma v> = C1 \cdot \theta \cdot \sqrt{\xi/(m_r c^2 T^3)} \cdot e^{-3\xi}, \tag{26}$$

$$\theta = T/[1 - \frac{T \cdot (C2 + T \cdot (C4 + T \cdot C6))}{1 + T \cdot (C3 + T \cdot (C5 + T \cdot C7))}], \tag{27}$$

$$\xi = (B_G^2/(4\,\theta))^{1/3}. \tag{28}$$

This fit was done with the SAS program package[SAS]. The resulting parameters are shown in Table 6. The reactivity $<\sigma v>$ is in cm^3/s when T is the ion temperature in keV. All the fits are valid for ion temperatures 0.2 keV $\leq T_i \leq$ 100 keV, and the maximum deviation of the fit formula from the input data is shown in the last line of the table.
Figure 38 shows the ratio of the parametrization to the input reactivity data as a function of the energy for the resonant reactions, while Figure 39 shows the same comparison for the non-resonant reactions.
The absolute uncertainties for the reactivities calculated from the R-matrix cross-sections are 3 % for the DT-reaction, 6 % for the DD-reactions, and 10 % for the D(^{3}He,p)α-reaction. Since the errors of the fit are negligible, these values are the the total errors of our parametrization.
For order of magnitude estimates table 7 shows the thermal reactivities as a function of the ion temperature. These values have been calculated with the fit parameters from table 6.

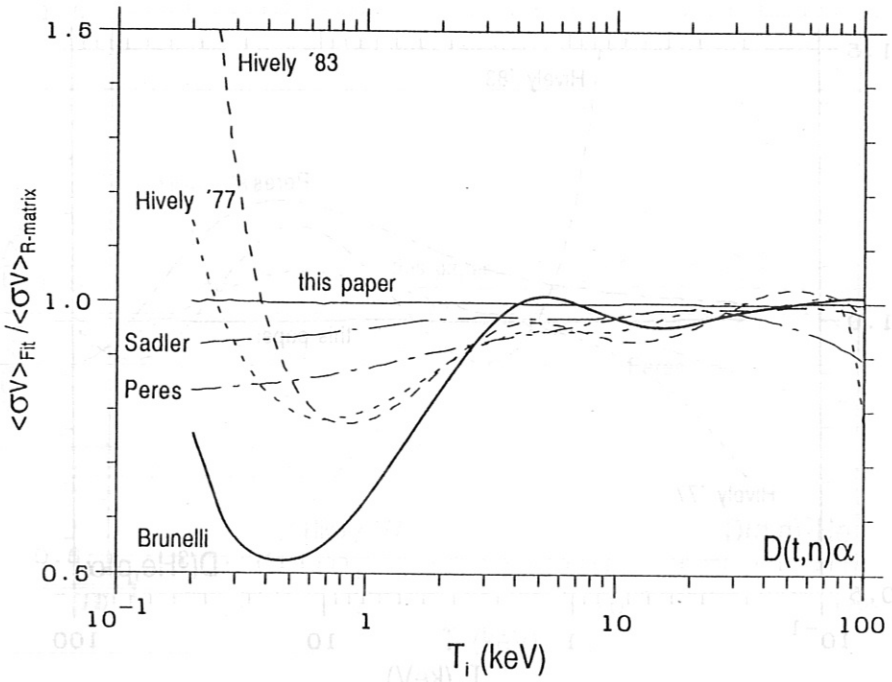

Figure 40: Comparison of different $<\sigma v>$ fit formulas with the reactivity values calculated from the R-matrix cross-sections for the D(t,n)α-reaction. For the curve labels see text.

5.3 Comparison with the old parametrizations

Next we compare this parametrization together with the old formulas with the original reactivity values calculated by G. M. Hale. Figure 40 shows this comparison for the D(t,n)α-reaction as the ratio of the values calculated from the fit formulas to the input data. Hively et al.[HIVELY77A, HIVELY83A] and Brunelli[BRUNELLI80A] used the reactivity data that Miley et al.[MILEY74A] calculated from Duane's cross-section formulas[DUANE72A]. The curve labeled "HIVELY '77" was calculated from equation (5) in Hively's 1977 paper[HIVELY77A]. All three of these parametrizations show large deviations from the correct reactivities for low ion temperatures, as one would expect from the fact that Duane's cross-section formulas were used. Peres's formula[PERES79A] is about 15 % too low at $T_i = 1$ keV but only 2 % too low for ion temperatures above 10 keV. Sadler's parametrization[SADLER87A], which is based on intermediate R-matrix results[JARMIE84A], is only about 5 % too low between 1 and 10 keV, but above 20 keV the deviation increases up to about 10 % at 100 keV.
Figure 41 shows the same comparison for the D(^{3}He,p)α-reaction. The problems we saw in Figures 9 to 13 with the cross-section formulas are also reflected in the reactivity parametrizations. The deviations are quite large and they even change sign.
For the D(d,p)T-reaction shown in Figure 42 the parametrization of Peres[PERES79A] is always better than 10 %, but again the formulas based on Duane's data[DUANE72A] have quite large deviations. In Figure 43 the comparison for the D(d,n)^{3}He-reaction shows the same situation for Hively's formulas, but Peres's formula has a much larger deviation (up to about 20 %) for high ion temperatures.

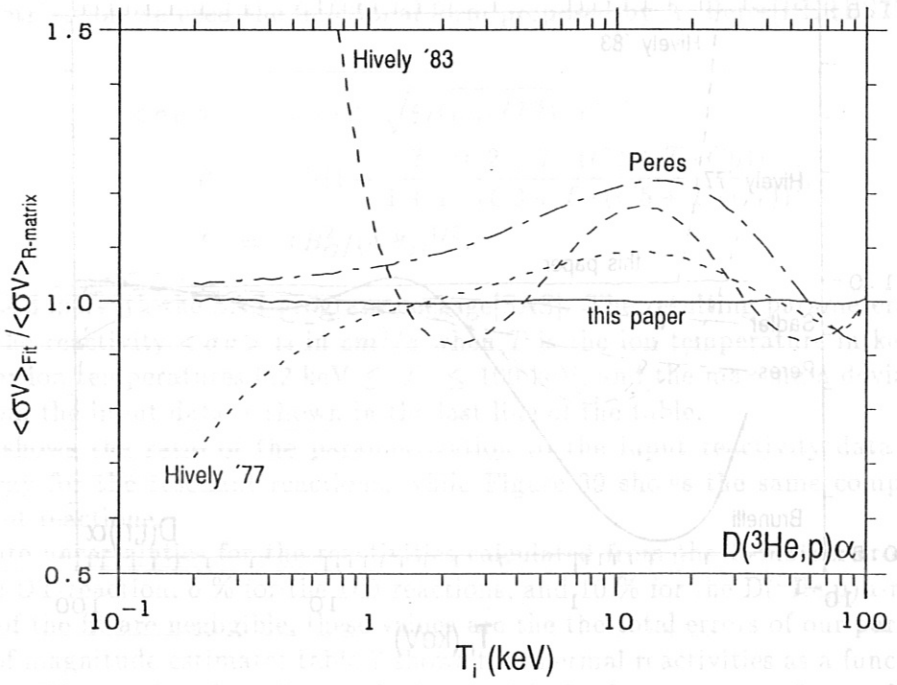

Figure 41: Comparison of different $< \sigma v >$ fit formulas for the D(^{3}He,n)α-reaction with the reactivity values calculated from the R-matrix cross-sections.

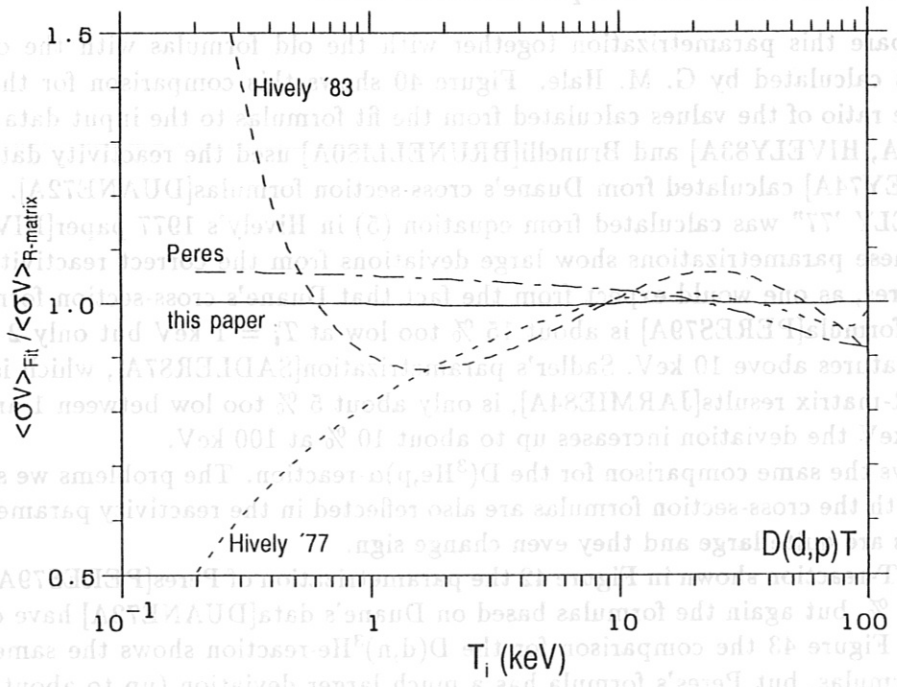

Figure 42: Comparison of different $< \sigma v >$ fit formulas for the D(d,p)T-reaction with the reactivity values calculated from the R-matrix cross-sections.

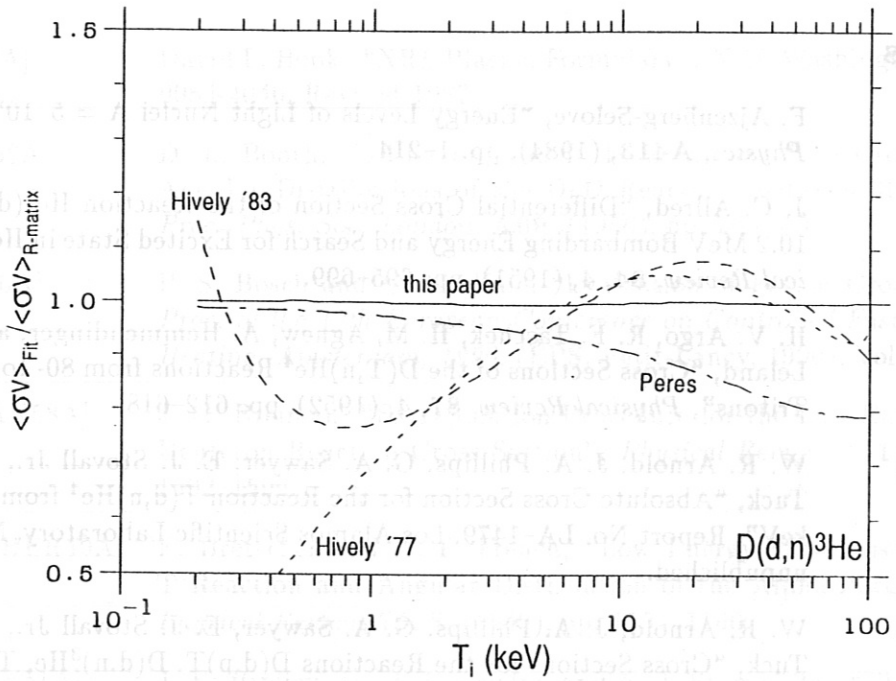

Figure 43: Comparison of different $< \sigma v >$ fit formulas for the D(d,n)^{3}He-reaction with the reactivity values calculated from the R-matrix cross-sections.

6 Acknowledgments

The author is grateful to G. M. Hale (LANL) for making unpublished R-matrix results available to perform the parametrizations in sections 4 and 5, and for many fruitful discussions.
He also acknowledges the useful discussions and contributions made by U. Schumacher, B. Bomba, and G. Sadler (JET). Thanks are also due to O. Kardaun for help with SAS, to J. Murphy (PPPL) for making the use of LOCUS possible at IPP, and to H. Volkenandt for her help in preparing the numerous figures.

References

[AJZEN84A] F. Ajzenberg-Selove, "Energy Levels of Light Nuclei A = 5–10", *Nuclear Physics*, **A413**, (1984), pp. 1–214.

[ALLRED51A] J. C. Allred, "Differential Cross Section of the Reaction $He^3(d,p)He^4$ at 10.2 MeV Bombarding Energy and Search for Excited State in He^4", *Physical Review*, **84**, 4, (1951), pp. 695–699.

[ARGO52A] H. V. Argo, R. F. Taschek, H. M. Agnew, A. Hemmendinger, and W. T. Leland, "Cross Sections of the D(T,n)He^4 Reactions from 80- to 1200-keV Tritons", *Physical Review*, **87**, 4, (1952), pp. 612–618.

[ARNOLD53A] W. R. Arnold, J. A. Phillips, G. A. Sawyer, E. J. Stovall Jr., and J. L. Tuck, "Absolute Cross Section for the Reaction T(d,n)He^4 from 10 to 120 keV", Report No. LA–1479, Los Alamos Scientific Laboratory, NM, 1953. unpublished.

[ARNOLD54A] W. R. Arnold, J. A. Phillips, G. A. Sawyer, E. J. Stovall Jr., and J. L. Tuck, "Cross Sections for the Reactions D(d,p)T, D(d,n)^{3}He, T(d,n)^{4}He, and ^{3}He(d,p)^{4}He below 120 KeV", *Physical Review*, **93**, 3, (1954), pp. 483–497.

[ASSEN87A] H. J. Assenbaum, K. Langanke, and C. Rolfs, "Effects of Electron Screening on Low-Energy Fusion Cross Sections", *Z. Phys. A - Atomic Nuclei*, **327**, (1987), pp. 461–468.

[BAHCALL66A] John N. Bahcall, "Non-Resonant Nuclear Reactions at Stellar Temperatures", *Astrophys. J.*, **143**, (1966), pp. 259–261.

[BALABANOV57A] E. M. Balabanov, I. Ia. Barit, L. N. Katsaurov, I. M. Frank, and I. V. Shtranikh, "Measurements of the Yields and Effective Cross Sections of the D(t,n)He^4 and D(d,p)T Reactions Using Thick Targets of Heavy Ice", *Supplement No. 5 of Sov. J. At. Energy, Atomnaya Energiya (1957)*, pp. 37–42.

[BALABANOV57B] E. M. Balabanov, I. Ia. Barit, L. N. Katsaurov, I. M. Frank, and I. V. Shtranikh, "Measurement of the Effective Cross Section for the D(t,n)He^4 Reaction in the Deuteron Energy Range 40-730 keV", *Supplement No. 5 of Sov. J. At. Energy, Atomnaya Energiya (1957)*, pp. 43–52.

[BAME57A] S. J. Bame Jr. and J. E. Peery Jr., "T(d,n)He^4 Reaction", *Physical Review*, **107**, 6, (1957), pp. 1616–1620.

[BLAIR48A] J. Morris Blair, George Freier, Eugene Lampi, William Sleator, Jr., and J. H. Williams, "The Angular Distributions of the Products of the D–D Reaction: 1 to 3.5 MeV", *Physical Review*, **74**, 11, (1948), pp. 1599–1603.

[BONNER52A] T. W. Bonner, J. P. Conner, and A. B. Lillie, "Cross Section and Angular Distribution of the $He^3(d,p)He^4$ Nuclear Reaction", *Physical Review*, **88**, 3, (1952), pp. 473–476.

[BOOK87A] David L. Book. "NRL Plasma Formulary". NRL Washington, publication 0084-4040, Revised 1987.

[BOOTH56A] D. L. Booth, G. Preston, and P. F. D. Shaw, "The Cross Section and Angular Distributions of the D–D Reactions between 40 and 90 keV", *Proc. Phys. Soc. London*, **A69**, (1956), pp. 265–270.

[BOSCH90A] H.-S. Bosch and G. M. Hale, "Evaluation of Fusion Cross-Sections", in *Proc. of the 17th European Conference on Controlled Fusion and Plasma Heating, Amsterdam, 1990*, (EPS, Petit-Lancy, 1990), Vol. IV, pp. 0–0.

[BRENNAN58A] J. G. Brennan, "Extrapolation Procedure for the Low-Energy Deuteron-Deuteron Reaction Cross Section", *Physical Review*, **111**, 6, (1958), pp. 1592–1596.

[BRETSCHER49A] E. Bretscher and A. P. French, "Low Energy Cross Section of the D–T Reaction and Angular Distribution of the Alpha-Particles Emitted", *Physical Review*, **75**, 8, (1949), pp. 1154–1160.

[BROLLEY51A] J. E. Brolley, Jr., J. L. Fowler, and E. J. Stovall, Jr., "The Angular Distribution of the Products of the T(D,n)He^4 Reaction", *Physical Review*, **82**, 4, (1951), pp. 502–505.

[BROLLEY57A] J. E. Brolley, Jr., T. M. Putnam, and Louis Rosen, "d-D Reactions at 6- to 14-MeV Input Energy", *Physical Review*, **107**, 3, (1957), pp. 820–824.

[BROWN86A] Ronald E. Brown and Nelson Jarmie, "Hydrogen Fusion-Energy Reactions", in Phillip G. Young et. al., editor, *Nuclear Data for Basic and Applied Science*, (Gordon and Breach, New York, 1986), Vol. 1, pp. 45–57.

[BROWN87A] E. Brown, Ronald, Nelson Jarmie, and G. M. Hale, "Fusion-Energy Reaction ^{3}H(d,α)n at Low Energies", *Physical Review*, **C 35**, 6, (1987), pp. 1999–2004. erratum in **36**, (1987) p.1220.

[BROWN89A] Ronald E. Brown and Nelson Jarmie, "Differential Cross Sections at Low Energies for ^{2}H(d,p)^{3}H and ^{2}H(d,n)^{3}He", *Physical Review*, **C 41**, 4, (1990), pp. 1391–1400. preprint in LA-UR-89-953, 1989.

[BRUECKNER74A] Keith A. Brueckner and Siebe Jorna, "Laser-driven Fusion", *Reviews of Modern Physics*, **46**, 2, (1974), pp. 325–367.

[BRUNELLI80A] B. Brunelli, "An Empirical Formula for the (D,T) Reaction Rate Parameter $< \sigma v >$", *Il Nuovo Cimento*, **55 B**, 2, (1980), pp. 264–267.

[BURBIDGE57A] E. Margaret Burbidge, G. R. Burbidge, William A. Fowler, and F. Hoyle, "Synthesis of the Elements in Stars", *Reviews of Modern Physics*, **29**, 4, (1957), p. 547.

[CECIL85B] F. E. Cecil, D. M. Cole, R. Philbin, Nelson Jarmie, and Ronald E. Brown, "Reaction $^{2}H(^{3}He,\gamma)^{5}Li$ at Center-of-Mass Energies between 25 and 60 keV", *Physical Review C*, **32**, 3, (1985), pp. 690–693.

[CECIL85C] F. E. Cecil, D. M. Cole, F. J. Wilkinson III, and S. S. Medley, "Measurement and Application of DDγ, DTγ and D^{3}Heγ Reactions at Low Energy", *Nuclear Instruments and Methods*, **B10/11**, (1985), pp. 411–414.

[CHAGNON56A] Paul R. Chagnon and George E. Owens, "Angular Distribution of the D+D Neutrons", *Physical Review*, **101**, 6, (1956), pp. 1798–1803.

[CLAYTON68A] D. D. Clayton, *Principles of Stellar Evolution and Nucleosynthesis*, McGraw-Hill, New York, (1968).

[CLAYTON74A] Donald D. Clayton and Stanford E. Woosley, "Thermonuclear Astrophysics", *Reviews of Modern Physics*, **46**, 4, (1974), pp. 755–771.

[CONNER52A] J. P. Conner, T. W. Bonner, and J. R. Smith, "A Study of the $H^{3}(d,n)He^{4}$ Reaction", *Physical Review*, **88**, 3, (1952), pp. 468–473.

[CORE87B] W. G. F. Core, "A Note on the Computation of Thermonuclear Reactivities in Plasma-Fusion Applications", Report No. JET-IR(87)11, JET, Culham, GB, 1987.

[DAVENPORT53A] P. A. Davenport, T. O. Jeffries, Maureen E. Owen, F. V. Price, and D. Roaf, "The D–D Cross-Section and Angular Distribution Between 55 and 430 keV", *Proc. Roy. Soc. London*, **A 216**, (1953), pp. 66–71.

[DAVIDENKO57A] V. A. Davidenko, A. M. Kucher, I. S. Pogrebov, and Iu. F. Tuturov, "Determination of the Total Cross Section for the $D(d,n)He^{3}$ Reaction in the Energy Region 20-220 keV", *Supplement No. 5 of Sov. J. At. Energy, Atomnaya Energiya (1957)*, pp. 7–12.

[DROSG87A] M. Drosg and O. Schwerer. "Production of Monoenergetic Neutrons between 0.1 and 23 MeV". in *Handbook on Nuclear Activation Data*, pp. 83–162. IAEA, Vienna, 1987.

[DUANE72A] B. H. Duane. "Fusion Cross Section Theory". in W. C. Wolkenhauer, editor, *Annual Report on CTR Technology 1972*. Batelle Pacific Northwest Laboratory, Richland, WS, 1972. BNWL-1685.

[ELIOT53A] Elizabeth A. Eliot, D. Roaf, and P. F. D. Shaw, "The Cross-Section and Angular Distribution of the D–D Reactions Below 50 keV", *Proc. Roy. Soc. London*, **A 216**, (1953), pp. 57–65.

[ENGEL61A] A. von Engel and C. C. Goodyear, "Fusion Cross-Section Measurements with Deuterons of low Energy", *Proc. Roy. Soc. London*, **A 264**, (1961), pp. 445–457.

[ENGSTLER88A] S. Engstler, A. Krauss, K. Neldner, C. Rolfs, U. Schröder, and K. Langanke, "Effects of Electron Screening on the ^{3}He(d,p)^{4}He Low-Energy Cross Sections", *Physics Letters*, **B 202**, 2, (1988), pp. 179–184.

[ERICKSON49A] K. W. Erickson, J. L. Fowler, and E. J. Stovall, Jr., "Cross Section as a Function of Angle for the D(d,n)He^3 Reaction for 10-MeV Bombarding Deuterons", *Physical Review*, **76**, 8, (1949), pp. 1141–1145.

[FIARMAN73A] S. Fiarman and W. E. Meyerhof, "Energy Levels of Light Nuclei A = 4", *Nuclear Physics*, **A206**, (1973), pp. 1–64.

[FICK73A] D. Fick and Ursula Weiss, "The (^{2}H–*d*)-Reactions below 200 keV", *Z. Physik*, **265**, (1973), pp. 87–104.

[FREIER54A] G. Freier and H. Holmgren, "Interaction between D^2 and He^3 in the Neighborhood of the 18.6-MeV Level of Li^{5*}", *Physical Review*, **93**, 4, (1954), pp. 825–826.

[FULLER57A] J. C. Fuller, W. E. Dance, and D. C. Ralph, "Angular Distribution of the D(d,n)^{3}He Reaction Below 1 MeV", *Physical Review*, **108**, 1, (1957), pp. 91–93.

[FUTCH72A] A. H. Futch, Jr., J. P. Holdren, J. Killeen, and A. A. Mirin, "Multi-Species Fokker-Planck Calculations for D-T and D-^{3}He Mirror Reactors", *Plasma Physics*, **14**, (1972), pp. 211–244.

[GALONSKY56A] A. Galonsky and C. H. Johnson, "Cross Sections for the T(d,n)He^4 Reaction", *Physical Review*, **104**, 2, (1956), pp. 421–425.

[GAMOV28A] G. Gamov, "Zur Quantentheorie des Atomkernes", *Zeitschr. Physik*, **51**, (1928), pp. 204–212.

[GANEEV57A] A. S. Ganeev, A. M. Govorov, G. M. Osetinskii, A. N. Rakivnenko, I. V. Sizov, and V. S. Siksin, "The D–D Reaction in the Deuteron Energy Range 100–1000 keV", *Supplement No. 5 of Sov. J. At. Energy, Atomnaya Energiya (1957)*, pp. 21–36.

[GOLDBERG60A] Murrey D. Goldberg and James M. Le Blanc, "Angular Distribution of the D(d,n)He^3 Reaction for 5- to 12-MeV Deuterons", *Physical Review*, **119**, 6, (1960), pp. 1992–1999.

[GOLDBERG61A] Murrey D. Goldberg and James M. Le Blanc, "Angular Yield of Neutrons from the T(d,n)He^4 Reaction for 6- to 11.5-MeV Deuterons", *Physical Review*, **122**, 1, (1961), pp. 164–168.

[GREENE67A] Samuel L. Greene, Jr., "Maxwell Averaged Cross Sections for some Thermonuclear Reactions on Light Isotopes", Report No. UCRL-70522, LRL, Livermore, CA, May 1967.

[HALE79A] G. M. Hale and D. C. Dodder, "R-Matrix Analyses of Light-Element Reactions for Fusion Applications", in J. L. Fowler, editor, *Proc. of the Int. Conf. on Nuclear Cross Sections for Technology, Knoxville, 1979*, (NBS, Washington, 1980), pp. 650–658. NBS special publication 594.

[HALE79B] Gerald M. Hale. "Data for Fusion Reactions". LASL memo T-2-L-3360, July 31, 1979, last updated Sept. 1986.

[HALE86A] Gerald M. Hale. "d-t Cross Section and Reaction Rate". LASL memo T-2-M-1767, September 17, 1986.

[HALE87A] G. M. Hale, Ronald E. Brown, and Nelson Jarmie, "Pole Structure of the $J^\pi = \frac{3}{2}^+$ Resonance in ^{5}He", *Physical Review Letters*, **59**, 7, (1987), pp. 763–766. comment in vol 59., pages 2818–2819.

[HALEPERS] G. M. Hale. LASL, private communication.

[HEMMEN55A] A. Hemmendinger and H. V. Argo, "Reaction D(t,α)n at 1.5 MeV", *Physical Review*, **98**, 1, (1955), pp. 70–72.

[HIVELY77A] L. M. Hively, "Convenient Computational Forms for Maxwellian Reactivities", *Nuclear Fusion*, **17**, 4, (1977), pp. 873–876.

[HIVELY83A] Lee M. Hively, "A Simple Computational Form for Maxwellian Reactivities", *Nuclear Technology/Fusion*, **3**, (1983), pp. 199–200.

[HUNTER49A] G. T. Hunter and H. T. Richards, "Yield and Angular Distribution of the D–D Neutrons", *Physical Review*, **76**, 10, (1949), pp. 1445–1449.

[ICHIMARU82A] Setsuo Ichimaru, "Strongly coupled plasmas: high-density classical plasmas and degenerate electron liquids", *Reviews of Modern Physics*, **54**, 4, (1982), pp. 1017–1059.

[JARMIE56A] N. Jarmie, J. D. Seagrave, R. C. Allen, A. Armstrong, H. V. Argo, S. J. Bame, J. E. Brolley, J. H. Coon, G. M. Frye, A. Hemmendinger, et al., "Charged Particle Cross Sections", Report No. LA-2014, LASL, Los Alamos, NM, March 1956.

[JARMIE81A] Nelson Jarmie, "Low-Energy Nuclear Fusion Data and their Relation to Magnetic and Laser Fusion", *Nucl. Sci. and Eng.*, **78**, (1981), pp. 404–412.

[JARMIE82A] Nelson Jarmie, Ronald E. Brown, and R. A. Hardekopf, "D(t,α)n Reaction Cross Sections at Low Energy", in K. H. Böckhoff, editor, *Proc. of the Int. Conf. on Nuclear Data for Science and Technology, Antwerpen, 1982*, (Reidel, Dordrecht, Nl, 1983), pp. 318–325.

[JARMIE84A] Nelson Jarmie, Ronald E. Brown, and R. A. Hardekopf, "Fusion-Energy Reaction ^{2}H(t,α)n from E_t = 12.5 to 117 keV", *Physical Review*, **C29**, 6, (1984), pp. 2031–2046. erratum in **C33** (1986), p. 385.

[JARMIE85A] Nelson Jarmie and Ronald E. Brown, "Low-Energy Nuclear Reactions with Hydrogen Isotopes", *Nuclear Instruments and Methods in Physics Research*, **B10/11**, (1985), pp. 405–410.

[JARMIE86A] Nelson Jarmie, "Requirements for Charged-Particle Reaction Cross Sections in the D–T, D–D, and D–^{3}He Fuel Cycles", in *Proc. of an Advisory Group Meeting on Nuclear Data for Fusion Reactor Technology, Gaussig, GDR, 1986*, (IAEA, Vienna, 1988), pp. 79–86. preprint in Los Alamos report LA-UR–86-3705.

[JARVIS53A] R. G. Jarvis and D. Roaf, "Comparison of D–T and D–^{3}He at Low Energies", *Proc. Roy. Soc. London*, **A 218**, (1953), pp. 432–438.

[JOHNER87A] J. Johner, "Optimized Monomial Approximations with Integer Exponents of the Deuterium-Tritium Thermonuclear Reaction Rate", Report No. EUR-CEA-FC-1320, C.E.N., Cadarache, February 1987.

[KATSAUROV62A] L. N. Katsaurov, "Investigations of the Reaction D(T,n)He^4 by the Thin-Target Method in the Energy Range from 40 to 750 keV", *Akad, Nauk, USSR, Trudy Fizicheskii Inst.*, **14**, (1962), pp. 224–262.

[KLIUCHAREV56A] A. P. Kliucharev, B. N. Esel'son, and A. K. Val'ter, "A Study of the Reaction of He^3 with Deuterons", *Sov. Phys. Dokl.*, **1**, (1956), pp. 475–477.

[KOBZEV66A] A. P. Kobzev, V. I. Salatskij, and S. A. Telezhnikov, "Differential Cross Sections for the Reaction D(t,α)n at 115–1650 keV", *Sovjet Journal of Nuclear Physics*, **3**, 6, (1966), pp. 774–776. Translation of J. Nucl. Phys. (U.S.S.R.) **3**, 1060-1063 (June, 1966).

[KOONIN89A] S. E. Koonin and M. Nauenberg, "Calculated Fusion Rates in Isotopic Hydrogen Molecules", *Nature*, **339**, (1989), pp. 690–691.

[KRAUSS87A] A. Krauss, H. W. Becker, H. P. Trautvetter, C. Rolfs, and K. Brand, "Low-Energy Fusion Cross Sections of D + D and D + ^{3}He Reactions", *Nuclear Physics*, **A465**, (1987), pp. 150–172.

[KUNZ55A] W. E. Kunz, "Deuterium He^3 Reaction", *Physical Review*, **97**, 2, (1955), pp. 456–462.

[LANE58A] A. M. Lane and R. G. Thomas, "R-Matrix Theory of Nuclear Reactions", *Reviews of Modern Physics*, **30**, 2, (1958), pp. 257–353.

[LISKIEN73A] Horst Liskien and Arno Paulsen, "Neutron Production Cross Sections and Energies for the Reactions $T(p,n)^3He$, $D(d,n)^3He$ and $T(d,n)^4He$", *Nuclear Data Tables*, **11**, (1973), pp. 569–619.

[MANNING42A] H. P. Manning, R. D. Huntoon, F. E. Myers, and V. J. Young, "Distribution in Angle of Protons from the D-D Reaction", *Physical Review*, **61**, (1942), pp. 371–374.

[MCNALLY79A] J. Rand McNally, Jr., K. E. Rothe, and R. D. Sharp, "Fusion Reactivity Graphs and Tables for Charged Particle Reactions", Report No. ORNL/TM-6914, ORNL, Oak Ridge, TN, August 1979.

[MCNEILL51A] K. G. McNeill and G. M. Keyser, "The Relative Probabilities and Absolute Cross Sections of the D–D Reactions", *Physical Review*, **81**, 4, (1951), pp. 602–606.

[MCNEILL55A] K. G. McNeill, "A Note on the Branching Ratio of the D-D Reactions", *Phil. Mag.*, **46**, (1955), pp. 800–804.

[MEDLEY85A] S. S. Medley, F. E. Cecil, D. Cole, M. A. Conway, and F. J. Wilkinson, III, "Fusion Gamma Diagnostics", *Review of Scientific Instruments*, **56**, 5, (1985), pp. 975–977.

[MIKKELSEN89A] D. R. Mikkelsen, "Approximation for Non-Resonant Beam Target Fusion Reactivities", *Nuclear Fusion*, **29**, 7, (1989), pp. 1113–1115.

[MILEY74A] George H. Miley, Harry Towner, and Nenad Ivich, "Fusion Cross Sections and Reactivities", Report No. COO-2218-17, University of Illinois, Urbana, IL, June 1974.

[MILONE61A] C. Milone and R. Ricamo, "Differential Cross-Section for the D(d,n) Reaction", *Il Nuovo Cimento*, **22**, (1961), pp. 116–122.

[MOELLER80A] W. Möller and F. Besenbacher, "A Note on the ^{3}He+D Nuclear-Reaction Cross Section", *Nuclear Instruments and Methods*, **168**, (1980), pp. 111–114.

[MOFFAT52A] J. Moffat, D. Roaf, and J. H. Sanders, "The D–D Cross-Section and Angular Distribution Below 50 keV", *Proc. Roy. Soc. London*, **A 212**, (1952), pp. 220–234.

[MORGAN86A] G. L. Morgan, P. W. Lisowski, S. A. Wender, Ronald E. Brown, Nelson Jarmie, J. F. Wilkerson, and D. M. Drake, "Measurement of the Branching Ratio ^{3}H(d,γ)/^{3}H(d,n) Using Thick Tritium Gas Targets", *Physical Review*, **C33**, 4, (1986), pp. 1224–1227.

[MURPHY88A] J. A. Murphy and R. M. Wieland, "LOCUS Database System", *Review of Scientific Instruments*, **59**, 8, (1988), pp. 1780–1782.

[NIIKURA90A] Setsuo Niikura and Masayuki Nagami, "Improvement of Fusion Reactivity and Fusion Power Multiplication Factor in the Presence of Fast Ions", *Fusion Engineering and Design*, **12**, (1990), pp. 467–480.

[PERES79A] Asher Peres, "Fusion Cross Sections and Thermonuclear Reaction Rates", *Journal of Applied Physics*, **50**, 9, (1979), pp. 5569–5571.

[POSPIECH75A] G. Pospiech, H. Genz, E. H. Marlinghaus, A. Richter, and G. Schrieder, "Reactions ^{2}H(d,p)^{3}H and ^{2}H(d,n)^{3}He below 150 keV", *Nucl. Phys.*, **A239**, (1975), pp. 125–133.

[MCNALLY79A] J. Rand McNally, Jr., K. E. Rothe, and R. D. Sharp, "Fusion Reactivity Graphs and Tables for Charged Particle Reactions", Report No. ORNL/TM-6914, ORNL, Oak Ridge, TN, August 1979.

[MCNEILL51A] K. G. McNeill and G. M. Keyser, "The Relative Probabilities and Absolute Cross Sections of the D–D Reactions", *Physical Review*, **81**, 4, (1951), pp. 602–606.

[MCNEILL55A] K. G. McNeill, "A Note on the Branching Ratio of the D-D Reactions", *Phil. Mag.*, **46**, (1955), pp. 800–804.

[MEDLEY85A] S. S. Medley, F. E. Cecil, D. Cole, M. A. Conway, and F. J. Wilkinson, III, "Fusion Gamma Diagnostics", *Review of Scientific Instruments*, **56**, 5, (1985), pp. 975–977.

[MIKKELSEN89A] D. R. Mikkelsen, "Approximation for Non-Resonant Beam Target Fusion Reactivities", *Nuclear Fusion*, **29**, 7, (1989), pp. 1113–1115.

[MILEY74A] George H. Miley, Harry Towner, and Nenad Ivich, "Fusion Cross Sections and Reactivities", Report No. COO-2218-17, University of Illinois, Urbana, IL, June 1974.

[MILONE61A] C. Milone and R. Ricamo, "Differential Cross-Section for the D(d,n) Reaction", *Il Nuovo Cimento*, **22**, (1961), pp. 116–122.

[MOELLER80A] W. Möller and F. Besenbacher, "A Note on the ^{3}He+D Nuclear-Reaction Cross Section", *Nuclear Instruments and Methods*, **168**, (1980), pp. 111–114.

[MOFFAT52A] J. Moffat, D. Roaf, and J. H. Sanders, "The D–D Cross-Section and Angular Distribution Below 50 keV", *Proc. Roy. Soc. London*, **A 212**, (1952), pp. 220–234.

[MORGAN86A] G. L. Morgan, P. W. Lisowski, S. A. Wender, Ronald E. Brown, Nelson Jarmie, J. F. Wilkerson, and D. M. Drake, "Measurement of the Branching Ratio ^{3}H(d,γ)/^{3}H(d,n) Using Thick Tritium Gas Targets", *Physical Review*, **C33**, 4, (1986), pp. 1224–1227.

[MURPHY88A] J. A. Murphy and R. M. Wieland, "LOCUS Database System", *Review of Scientific Instruments*, **59**, 8, (1988), pp. 1780–1782.

[NIIKURA90A] Setsuo Niikura and Masayuki Nagami, "Improvement of Fusion Reactivity and Fusion Power Multiplication Factor in the Presence of Fast Ions", *Fusion Engineering and Design*, **12**, (1990), pp. 467–480.

[PERES79A] Asher Peres, "Fusion Cross Sections and Thermonuclear Reaction Rates", *Journal of Applied Physics*, **50**, 9, (1979), pp. 5569–5571.

[POSPIECH75A] G. Pospiech, H. Genz, E. H. Marlinghaus, A. Richter, and G. Schrieder, "Reactions ^{2}H(d,p)^{3}H and ^{2}H(d,n)^{3}He below 150 keV", *Nucl. Phys.*, **A239**, (1975), pp. 125–133.

[PRESTON54A] G. Preston, P. F. D. Shaw, and S. A. Young, "The Cross-Sections and Angular Distributions of the D–D Reactions between 150 and 450 keV", *Proc. Roy. Soc. (London)*, **A226**, (1954), pp. 206–216.

[ROTH90A] J. Roth, R. Behrisch, W. Möller, and W. Ottenberger, "Fusion Reactions During Low Energy Deuterium Implantation into Titanium", *Nuclear Fusion*, **30**, 3, (1990), pp. 441–446.

[RUBY63A] L. Ruby and R. B. Crawford, "Anisotropy Factors for the Determination of Total Neutron Yield from the D(d,n)^{3}He and T(d,n)^{4}He Reactions", *Nuclear Instruments and Methods*, **24**, (1963), pp. 413–417. Lawrence Radiation Laboratory Report UCRL-10752 Suppl. (1963).

[SADLER87A] G. Sadler, O. N. Jarvis, P. van Belle, N. Hawkes, and B. Syme, "Observation of Fusion Reaction γ-Rays in JET", in *Proc. of the 14th European Conference on Controlled Fusion and Plasma Physics, Madrid, 1987*, (EPS, Petit-Lancy, 1987), Vol. III, pp. 1232–1235.

[SADLER87B] G. Sadler and P. van Belle, "An Improved Formulation of the D(t,n)^{4}He Reaction Cross-Section", Report No. JET-IR(87)08, JET, Culham, 1987.

[SALPETER54A] E. E. Salpeter, "Electron Screening and Thermonuclear Reactions", *Austral. J. Phys.*, **7**, (1954), pp. 373–388.

[SAS] SAS. User's Guide: Statistics, SAS Institute Inc., Cary NC (1985).

[SCHIFF49A] Leonard I. Schiff, *Quantum Mechanics*, McGraw-Hill, New York, (1949). First edition, page 117.

[SCHULTE72A] R. L. Schulte, M. Cosack, A. W. Obst, and J. L. Weil, "^{2}H+d Reactions from 1.96 to 6.20 MeV", *Nuclear Physics*, **A192**, (1972), pp. 609–624.

[SLAUGHTER83A] Dennis Slaughter, "Fusion Reactivities for Several Beam and Target Ion Distributions", *Journal of Applied Physics*, **54**, 3, (1983), pp. 1209–1217.

[SMITH72A] J. R. Smith and S. T. Thornton, "Measurements of ^{3}H(d,$\vec{n}$)^{4}He Neutron Polarizations for E_d = 1.0 to 5.0 MeV", *Nuclear Physics*, **A187**, (1972), pp. 433–445.

[STEWART60A] L. Stewart, J. E. Brolley, Jr., and L. Rosen, "Interaction of 6- to 14-MeV Deuterons with Helium Three and Tritium", *Physical Review*, **119**, 5, (1960), pp. 1649–1653.

[STEWART74A] Leona Stewart and Gerald M. Hale, "The T(D,n)^{4}He and T(t,2n) Cross Sections at Low Energies", Report No. LA-5828-MS, LASL, Los Alamos, NM, December 1974.

[STRATTON52A] T. F. Stratton and George D. Freier, "The Angular Distribution of Alpha-Particles from the Reaction of Deuterons with Tritons", *Physical Review*, **88**, 2, (1952), pp. 261–263.

[THEUS66A] R. B. Theus, W. I. McGarry, and L. A. Beach, "Angular Distributions and Cross-Section Ratios for the Reactions ^{2}H(d,n)^{3}He And ^{2}H(d,p)^{3}H Below 500 keV", *Nuclear Physics*, **A80**, (1966), pp. 273–288.

[THIELE86A] Friedrich-Karl Thielemann and James W. Truran, "General Implementation of Screening Effects in Thermonuclear Reaction Rates", Report No. MPA 261, MPI for Physics and Astrophysics, Garching, FRG, September 1986.

[THORNTON69A] S. T. Thornton, "The D(d,n)^{3}He Reaction from E_d = 5 to 10 MeV", *Nuclear Physics*, **A136**, (1969), pp. 25–34.

[TUCK54A] James L. Tuck, "Thermonuclear Reaction Rates", Report No. LAMS–1640, LANL, Los Alamos, NM, March 1954.

[TUCK61A] J. L. Tuck, "Thermonuclear Reaction Rates", *Nuclear Fusion*, **1**, 2, (1961), pp. 201–202.

[WANDEL59A] C. F. Wandel, T. Hesselberg Jensen, and O. Kofoed-Hansen, "A Compilation of Some Rates and Cross Sections of Interest in Controlled Thermonuclear Research", *Nuclear Instruments and Methods*, **4**, (1959), pp. 249–260.

[WAPSTRA71A] A. H. Wapstra and N. B. Gove, "The 1971 Atomic Mass Evaluation", *Nuclear Data Tables*, **9**, (1971), pp. 265–468.

[WENZEL52A] W. A. Wenzel and Ward Whaling, "Cross Section and Angular Distribution of the D(d,p)T Reaction", *Physical Review*, **88**, 5, (1952), pp. 1149–1154.

[WILKINSON85A] F. J. Wilkinson III and F. E. Cecil, "^{2}H(d,γ)^{4}He Reaction at Low Energies", *Physical Review C*, **31**, 6, (1985), pp. 2036–2040.

[YARNELL53A] J. L. Yarnell, R. H. Lovberg, and W. R. Stratton, "Angular Distribution of the Reaction He^3(d,p)He^4 between 240 keV and 3.56 MeV", *Physical Review*, **90**, 2, (1953), pp. 292–297.